Response of cave microclimates to external atmospheric forcing

Processes and implications investigated in Totes Gebirge, Austria

Original abstract

An investigation into the role of condensation in alpine cave microclimates carried out in the Northern Calcareous Alps, Austria. This project builds on work carried out in Russia and the Ukraine since the 80s, and addresses the ongoing debate. Data will be collected via a network of atmospheric sensors placed on the surface and underground. Condensation will then be estimated from data and spatial distributions analysed and verified by visual and experimental observation of condensation related features and condensation itself. Discussion will explore connections with speleogenesis, karst water balance, "cave breathing," and cave thermal inertia (response to climate change).

Statement

This document is essentially my own unaided work, and support I received has been documented in the Acknowledgements and Preface. It does not exceed 10,000 words.

Acknowledgements

Preface

Cambridge University Caving Club's (CUCC) expeditions to Austria have been exploring a patch of the Austrian Alps, Kataster Area 1623, by permission of the Austrian Landesreigerung since 1976. Thanks to the continued cooperation of the government and local caving organisations, the expedition has developed a strong infrastructure (hardware, software, and "wetware") and as Expedition Leader I felt that the time was right in 2007 to add scientific objectives to our previously exploration-dominated leadership. Everyone involved with the expedition enthusiastically embraced the microclimate monitoring project, along with with Djuke Veldhuis' study of physiological stress in cavers and Professor Mark Dougherty's tests of new radon detectors. Expedition members showed their support by assisting in the planning and execution of the research. Although I also collected data from English caves, I decided that the initially planned comparative discussion would not provide scope for an in-depth analysis of the Austrian data.

I presented results of the microclimate project in their early stages of analysis at Hidden Earth 2007 and the BCRA Cave Science Symposium 2007. Preliminary reports were submitted to the CSTRI and RGS shortly after returning from the expedition. A general report on the expedition, including expedition and science goals, was published in (The present author, 2007).

Helpful feedback from many at the Symposium have influenced the content of this document, especially the suggestions of Chris Self regarding mechanisms for condensation removal. After the conference Gina Molesley referred me to Professor Mark Luetscher at Bristol, with whom I discussed via email the thermal effects of subterranean ice and who was kind enough to send me a relevant article in advance of its printing. Likewise, Professor Christoph Spötl at Innsbruck University provided an overview of microclimatic investigations in my area and commented on my research. Early on, Dr Neville Michie explained the many difficulties and pitfalls of obtaining useful cave microclimate data, and informed the initial planning of the monitoring scheme and purchase and construction of equipment.

The majority of the software used in this project is free and open source, and some of it was written by members of CUCC. Centrelines were calculated from survey data using Survex, and cave maps were produced using Tunnel (both are programs developed by CUCC members, now in common use internationally). All equipment was surveyed to from existing survey points to BCRA Grade 5e using the SAP electronic compass / clinometer developed by Phil Underwood (again, of CUCC). The document is typeset in LaTeX using BibTeX for referencing.

Contents

List of Figures

List of Tables

1 Introduction

1.1 Aims

This study seeks to characterise the heat flux between the caves investigated and the surface in terms of the relative magnitude of its component processes. Viewing the cave entrance as a plane, the heat flux Q_{Ent} across that surface is expected to be the sum of the flux of three types of heat transfer across that plane. These are the advective sensible heat flux Q_S, the advective latent heat flux Q_L, and the conductive heat flux Q_C through limestone, such that

$$Q_{Ent} = Q_C + Q_S + Q_L \tag{1}$$

The relative importance of these components is assessed here using data from simultaneous datalogged measurements of cave and surface atmospheric variables, as well as visual observation by a team of cavers. To begin with, the importance of the conductive flux Q_C is investigated. Because Q_C cannot be measured directly, I test a theory which assumes all heat transfer in caves is via Badino (2004)'s penetration legnth model by observing the distance from entrances at which diurnal temperature cycles are no longer visible. This zone of diurnal temperature variation is commonly referred to as the "heterothermic zone" (Luetscher & Jeannin, 2004). Evidence that Q_C alone is a very small component of heat transfer through the caves leads to a discussion of airflow through the cave and the "chimney effect" (Michie, 1997), representing Q_S. Likely latent heat flux (Q_L) is addressed through wet and dry bulb measurements of atmospheric water vapour content and visual observation of condensation. Existing theories are critically evaluated in the light of our data, to develop a conceptual model of heat transfer with empirical limits based on our observations.

1.2   Some background on cave microclimatology

An understanding of subsurface atmospheric conditions is vital for nearly every cave-related investigation. Cave climate is largely forced by surface[1] conditions, in a complicated and nonlinear manner (Figure 1). The speleogenesis of a cave, the development of calcite formations (Dreybrodt, Gabrov Ek, & Perne, 2005), its ability to act as an archive of climate history (e.g., Baker et al., 2007; Spötl, Fairchild, & Tooth, 2005; Fairchild & McMillan, 2007) or a habitat for unique species of life (Chapman, 1993) are all dependant on its microclimate. Even archaeological and anthropological studies often require knowledge of how the cave atmosphere responds to surface climates for understanding the preservation of rock art and artifacts (Hall, Meiklejohn, & Arocena, 2007). Within the scope of this dissertation, however, I will explicitly discuss only the implications for palaeoclimate studies (introduced in Section 2.2) and cave exploration.

Until recently, the majority of attempts to characterise surface-subsurface microclimatic coupling in caves have been either theoretical, or motivated by the maintenance of show caves or the conservation of cavernicoles (organisms which spend at least some of their lifecycle in caves) (Table 1). However, in the last two decades there have been some experimental studies of specific microclimatic processes, including condensation, and on the response of caves to climate change. I will introduce these authors in more depth while discussing specific processes. To the best of my knowledge, the present study is unique as the only cave microclimatic project in the Alps to examine condensation, and the only subsurface monitoring project in the Northern Alps of Austria.

---

[1]The term "surface" is used throughout this dissertation to signify "above ground." Interfaces between air, rock, and water are referred to as "boundary layers."
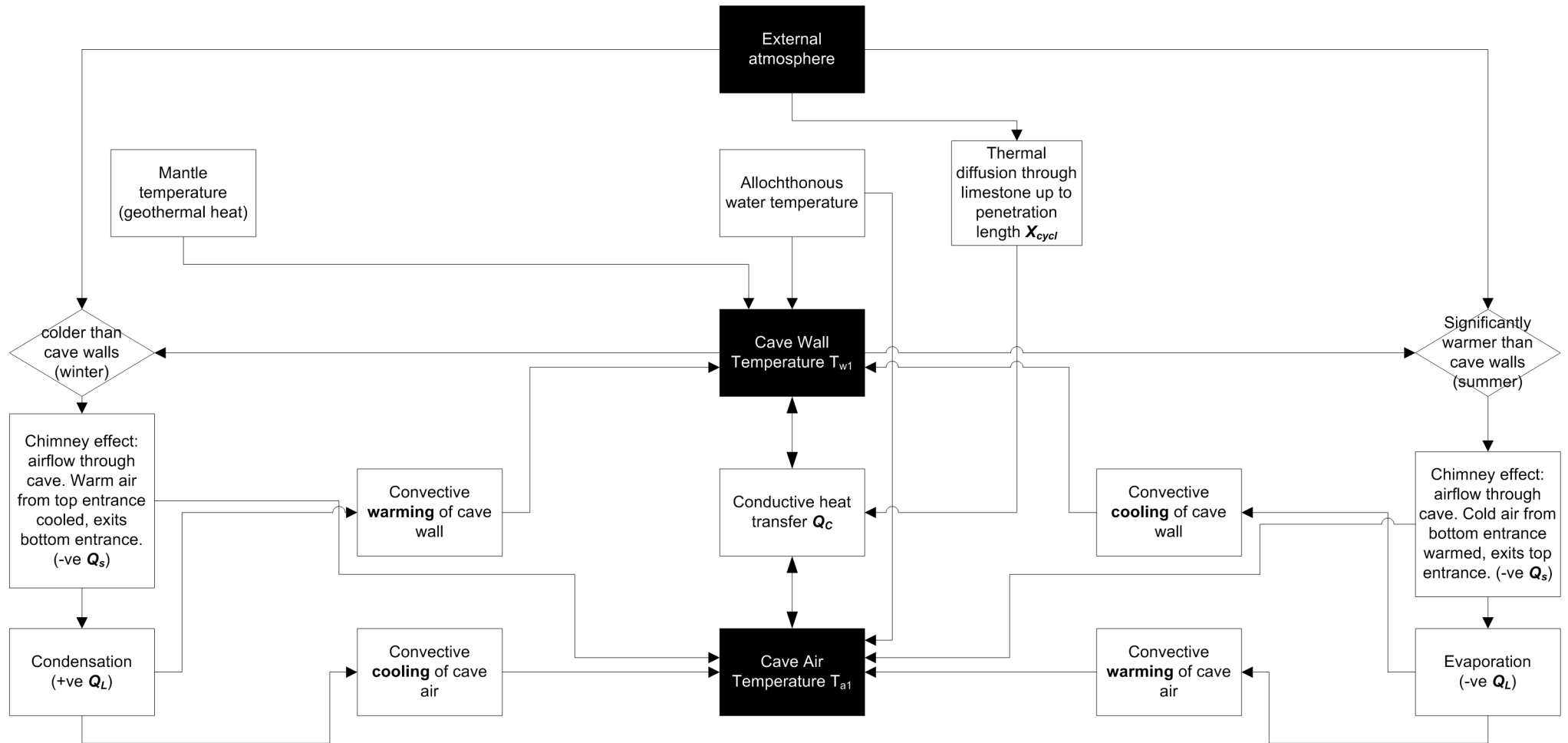
Figure 1: Schematic overview of major processes acting in cave microclimates

2 Geographical and academic setting

It is impossible to measure the great variety of microclimates by building an ever more dense network of observing stations. Moreover, since the essential characteristics of microclimates are repeated everywhere, it suffices to study them in special experimental areas.

(Geiger, 1950)

2.1 Special experimental areas

Research so far into external atmospheric influences on cave conditions has highlighted processes which are affected heavily by climatic variations with latitude and altitude (Dublyansky & Dublyansky, 1998). As a result, the dominant influences on cave microclimate vary geographically. Seasonal variation is also crucial, as a separate set of processes occur in summer and winter. In all three of these dimensions (latitude, altitude, and season), our study site is situated at a point extremely conducive to condensation. At 47°N, 1730m above sea level, in July through August, Dublyansky and Dublyansky (1998) predict the highest rates of condensation, up to 12g of condensate for each m^3 of air transported into the cave.

Although there are 172 caves accessible from the expedition Top Camp (listed at http://cucc.survex.com/expo/smkridge/), two caves were identified in which heterothermic zone microclimatic processes could be isolated; Rundreisehöhle and Steinbrückenhöhle. Rundreisehöhle was selected for its simple geometry. It stands alone in the area as the only cave of over 10m length with exactly two entrances. Its simple "tunnel" structure should lead to a single airflow pathway with relatively little leakage to or from side passages. Steinbrückenhöhle, on the other hand, is an extremely complex cave system in which exploration is ongoing. In Steinbrückenhöhle, research and exploration trips could be combined. It was typical, for example, to download data from loggers on the way to or from the pushing front. Three transects near entrances, each approximating a single airflow pathway with no major turnoffs, were monitored according to the protocol described in Section 3.

Near-simultaneous investigation of two caves of different scales is useful in the light of Heaton (2005, cited in Michie, 1997)'s findings that different microclimatic processes operate in caves of different sizes. A wind-tunnel effect specific to Rundreisehöhle is investigated in Section 5.2.1. It is shown below that due to Rundreisehöhle's short extent, diurnal variations affect the entire cave, i.e. there is no homothermic zone. Therefore it is only possible to observe the termination of the heterothermic zone in Steinbrückenhöhle. Condensation was not observable in Rundreisehöhle. Appendix B shows the areas chosen with a brief explanation and Table 2 summarises the data obtained.
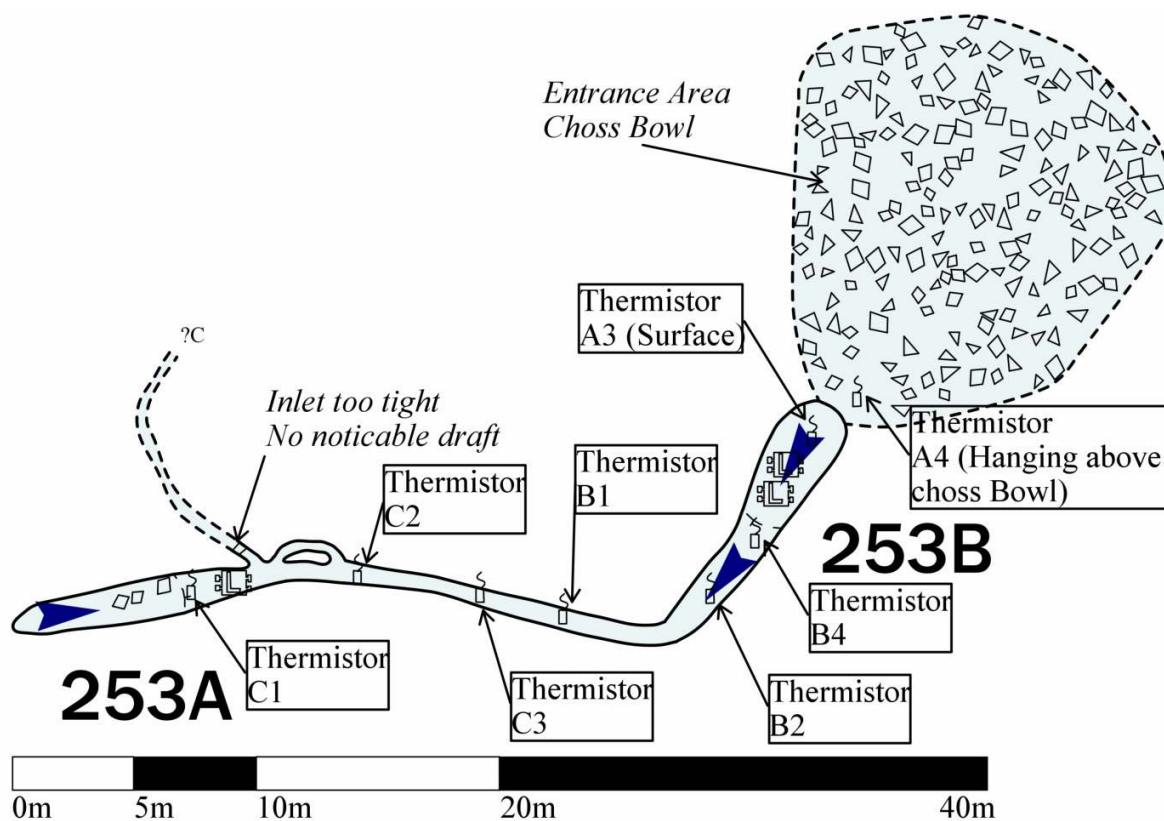
Figure 2: Survey of Rundreisehöhle (1623/253), annotated with sensor placements for data collection. 253A and B are entrances, and ?C denotes an extremely tight passage which has not been explored. Weather station was placed on the surface above 253B. North is up, see Figure 3 for Key.

2.2 Relevance to palaeoclimate studies

To understand the importance of this project for palaeoclimate studies, it is necessary to briefly discuss the aspects of speleothem elemental and isotopic composition which

15
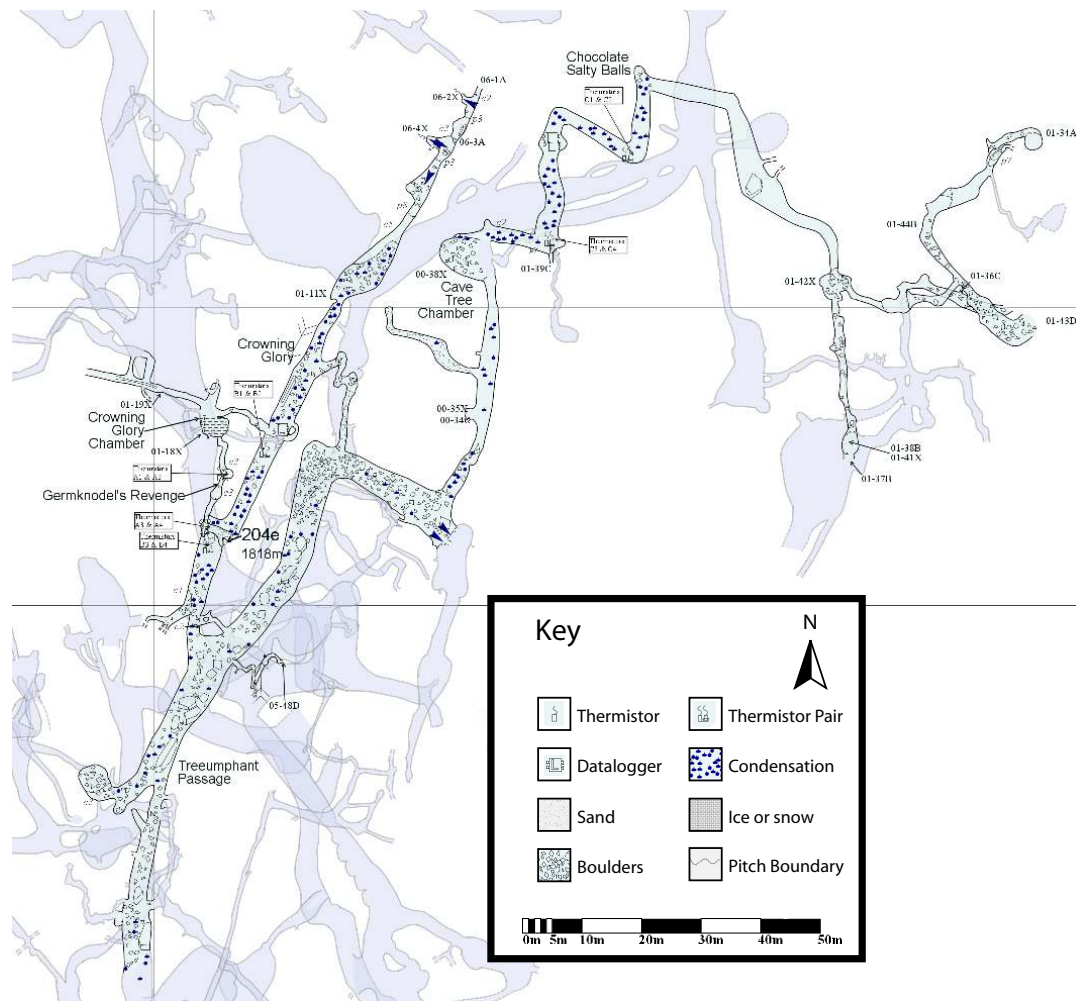
Figure 3: Survey of Steinbrückenhöhle, annotated with sensor placements for data collection, and extent of observed condensation.

have been used as palaeoclimate proxies. These proxies can be divided into two broad categories: those which are interpreted as indicators of surface conditions, and those which represent cave conditions directly. In the former case, understanding the surface-subsurface climatic coupling allows the application of the proxy to the surface. In the latter, subsurface conditions are often a secondary input to the signal which must be be accounted for. For these reasons, Verheyden (2005) called for further work to elucidate transfer functions between local cave climatology, surface conditions, and geochemistry. This study seeks to investigate some of these relationships in an alpine context.

The bulk of speleothem palaeoclimate research has approached deposition chemistry as a function of dripwater chemistry and thus of surface rather than subsurface conditions (Auler & Smart, 2004). This approach commonly requires controlling for subsurface microclimatology, as the environment of deposition is a significant secondary factor

16

on fractionation of δ^{18}O, δ^{18}D, and δ^{14}C. The calcite-water fractionation equation of (O'Neil, Clayton, & Mayeda, 1969) represents fragmentation as a function of the square root of temperature. More recent elaborations of this equation such as Lauritzen and Lundberg (1999) speleothem delta function (SDF) still include a crucial temperature term.

Evaporation and condensation processes may affect the rate of deposition by reducing the drip rate, and this is one source of annual lamination in speleothem (Fairchild et al., 2006), which provides the chronology for some proxy datasets. Microclimatic changes may affect the partial pressure of CO_2, also changing the rate of speleothem deposition (Spötl et al., 2005).

According to Oke (1998, p. 48), the relationship between the penetration length of two cyclicities, for example γ_{day} and γ_{year} can be estimated as:

$$\sqrt{\frac{\gamma_{day}}{\gamma_{year}}} \tag{2}$$

This would imply that the annual variation should extend around 19 times further into the cave than the diurnal variation. If valid for caves, this relationship could also be used for calculating the penetration length of longer scale cycles such as sunspot maxima / minima and glacial cycles. Therefore, testing of this relationship in caves could inform palaeoclimate studies and allow researchers to effectively choose which periodicity to focus on by using the cave frequency filter as a tool.

Some recent palaeoclimate studies have recognised the importance of monitoring cave microclimates, and incorporated such measurements into their results. At Rukiessa cave, Ethiopia, Baker et al. (2007) used datalogged temperature measurements and handheld humidity measurements in tandem with nearby surface weather stations to enable the inference of past rainfall from calcite δ^{18}O. However, the cave climate aspect of such studies is often neglected. Fairchild et al. (2006), for example, bemoans that

> There has been a relative neglect of the processes of air circulation in caves, an essential part of their physiology.

Where the effects of cave microclimatic processes are considered, the instruments and methods employed often lack the sensitivity to return meaningful results. Baker et

al. (2007) measured humidity at Rukiessa using handheld Kestrel devices, which, as they themselves stated, produce meaningful results to an "upper measurement limit of 95%." Two pages later, they report that their humidity results "averaged 97±2%." Micro-climatic investigations involved with cavernicole habitats or conservation of showcaves, such as Freitas and Schmekal (2003) and Michie (1997) tend to employ more effective equipment and cautious methodology. The present study aims to address processes that have been neglected in palaeoclimate studies, and to develop and carefully test an accurate monitoring system.

3 Methods and equipment

The necessity for working in small spaces requires the creation of a special field of instrumentation.

(Geiger, 1950)

3.1 Sensing air temperature

All underground temperatures measured in this study were sensed by HOBO TMC50-HD thermistors, which come from the company sealed and calibrated, resolving lower than 0.01℃ and with an absolute accuracy below 0.25℃. This instrumentation is similar to that of Kennedy (1998) but has greater precision and accuracy. The thermistors were hung in the centre of cave passages from protrusions on rock. Rock temperatures were not directly measured. The work of Michie (1997) suggests that cave air temperature is the most characteristic variable of the system in most cave microclimates.

3.2 Sensing airflow

3.2.1 Computational simulation

All data collected in this study are in transects running from an entrance into the cave. However, this is a one-dimensional approach and cave processes operate in three dimensions. For this reason, special consideration must be taken with the placement of sensors in a cross-section of passage. To create a representative picture of cave airflow using a one dimensional transect of anemometers and thermistors, a consistent scheme of placement is required. Ideally, they would be placed at the point of maximum or average flow for the cross-section which they monitor.

To achieve this, we used computational fluid dynamic (CFD) modeling of expected scenarios to evaluate likely cross-sectional variation before embarking on the expedition. Survey data collected by the 2004 Cambridge University Caving Club expedition at Rundreisehöhle was used to produce a 3D representation of the cave in StarFlow, a CFD package. The model created was an extremely simplified version of the cave. It

| Reference | Cave(s)investigated | Motivation | | | | Investigated | | | | | |
		Show cave maintenance	Cavernicole conservation	Theoretical process model	Climate change	Temperature	Humidity	Condensation	Airflow	Dust	CO_2
Cigna (1968)	N/A			X		X			X		
Fernández-Cortés, Calaforra, Jiménez-Espinosa, and Sánchez-Martos (2006)	Covadura system, Sorbas, Spain	X				X					
Freitas and Schmekal (2006)	Glowworm cave, New Zealand	X				X	X	X	X		
Stoeva and Stoev (2005)	Ledenika, Saeva dupka, Snezhanka and Uhlovitsa caves, Bulgaria	X			X						
Luetscher and Jeannin (2004)	20+ caves and tunnels from three continents			X		X			X		
Kennedy (1998)	Great scott, Bat, Saltpetre, Mammoth caves, and others, all in USA	X	X			X			X		
Dublyansky and Dublyansky (1998)	22 in the Crimea and the Caucasus			X				X			
Michie (1997)	Jenolan Caves, New South Wales	X		X		X	X	X	X	X	X
Forbes (1998)	Torgac Cave, New Mexico, USA	X				X	X				

Table 1: A selection of influential and recent cave microclimatic investigations.

consisted of only centreline and left-right-up-down (LRUD) data. A series of rhombuses were created to the dimensions described by the four LRUD values for each centreline point. Each rhombus was translated and rotated from the previous rhombus to follow the centreline. To convert this series of quadrilaterals into a volumetric space, a surface was "lofted" around the rhombuses.

A pressure difference was then set between the entrances, and the StarFlow simulation was run. The simulation works by dividing the volume into thousands of discrete cells and approximating the flow of air from each cell to the next. The results (Figure 4) showed that in some places, a single cross-section could easily give readings of up to a factor of ten apart depending upon where the anemometer was placed along that plane.
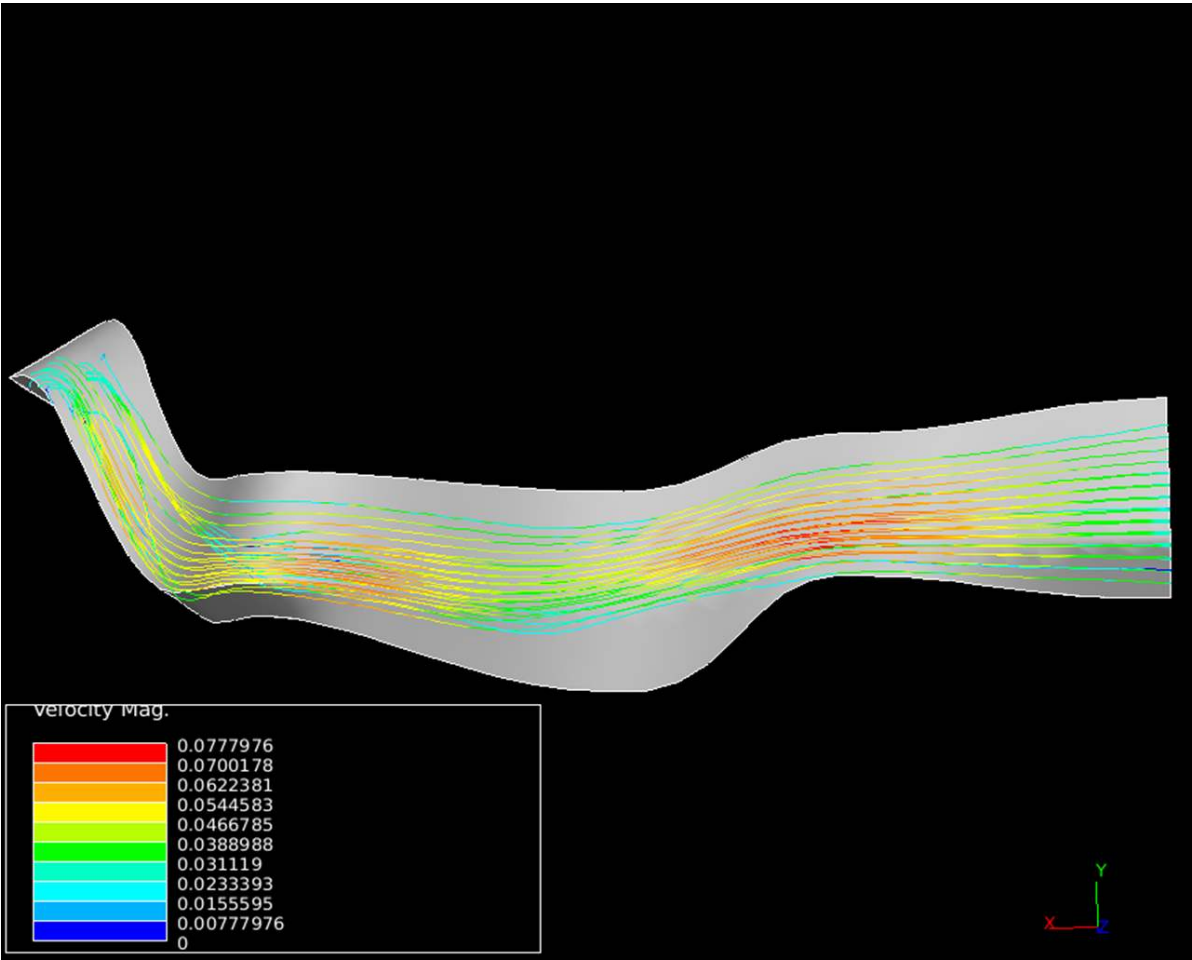
Figure 4: Computational fluid dynamics model for a pressure difference between the two entrances of Rundreisehöhle, produced using StarFlow

3.2.2 Equipment

Airflow in caves is generally very slow, well under 1m s^{-1}. Freitas and Schmekal (2006) measured a maximum value in Glowworm Cave of 0.16m s^{-1}. Conventional rotating vane anemometers are useless in this situation, so another method of airflow measurement was sought. Hot-wire anemometers are highly sensitive, but are unsuitable for this study because of their high power consumption and inability to detect flow direction (Lomas & Korman, 1990). An ultrasonic anemometer such as that outlined by Campbell and Unsworth (1979) appeared appropriate, but modern commercial models were prohibitively expensive. However, it is possible to construct such devices inexpensively using off-the shelf electronics (Michie, personal communication, 2007). I constructed two such devices (Appendix C). They were indeed capable of registering sufficiently small airflows. However, they require very exact calibration of the distance between the two transducers (which must be a multiple of the signal wavelength). Calibration requires an oscilloscope and therefore could not be conducted underground. Our hardware design proved not to be robust enough to maintain the calibration during transport into a cave and therefore no subsurface airflow data was produced. The devices will be improved for deployment in Summer 2008.

3.3 Sensing Humidity

Humidity can be measured by observing the difference between two thermometers (thermistors, in this case), if one of them is kept dry and the other one is exposed to the highest possible rate of evaporation. When exposed to sufficient evaporation the "wet bulb" thermistor tends towards a temperature known as dew point, which is the temperature above which water evaporates, and below which water condenses. Because the dew point is a function mainly of the moisture content of the air, comparing the actual temperature and the dew point temperature allows us to ascertain humidity.

In the course of this project, this principle was employed in the construction of two types of humidity measuring instrument. The first of these are simple wet / dry thermistor pairs, and the second is the micropsychrometer, which we used for spot mea-

surements. First I will explain the construction and calibration of the simple thermistor pairs.

Wet wicks were added to half of the sensors by sewing a thin piece of stretchy cotton fabric onto the metal thermistor head. During initial testing, the wicks were extended below the surface of water reservoirs (I experimented with plastic bags full of water, and hard plastic pots). However, for use in the highly humid underground environment, it was found that so little water evaporated that the wicks themselves were a sufficient water reservoir, so no plastic water bags or water pots were required. Because the wicks dried upwards, starting at the end furthest from the thermistor, there is no reason to believe that the evaporation rate was reduced with drying.
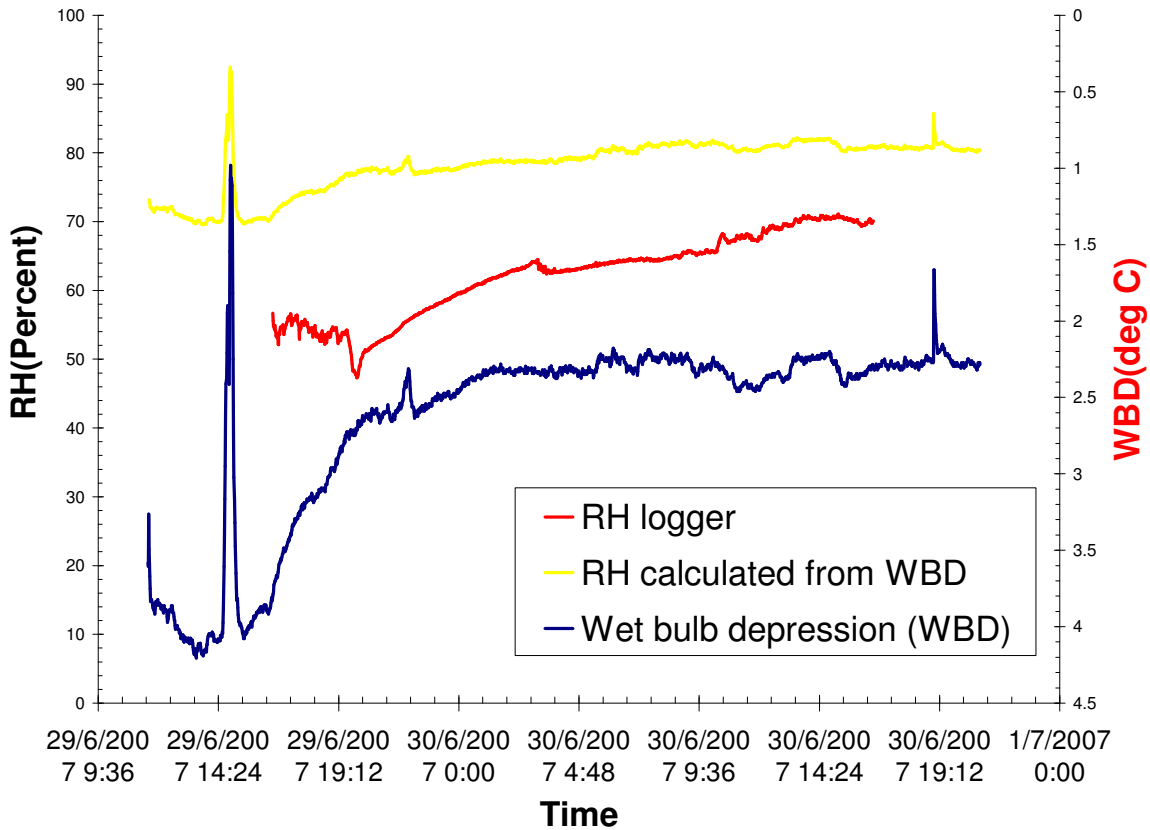
Figure 5: Testing / calibration of wet / dry bulb pairs with conventional RH sensor in CU Caving Club Tackle store

Calibration of the sensors occurred in the attic of the CU Caving Club tackle store. One dry bulb thermistor and two wet bulb thermistors were suspended from the attic ceiling in close proximity, and their output was logged every minute for six days. Control

data were provided by a conventional, thin-film capacitive humidity sensor and logged, also once per minute by an Easysense 100 series datalogger. Humidity variations reflected weather and also the presence of wet caving suits hanging to dry in the room below. Figure 5 shows the results of this initial calibration run. Subtracting the wet bulb temperature from the dry bulb temperature gives the wet bulb depression (WBD). The blue line on the graph in Figure 5 is the average of the WBD from the two wet bulb sensors.

The two methods of humidity measurement correlate to p=0.00. Although the majority of the data seem largely to agree, there appear to be data artifacts of some sort. To find a calibration equation (linear regression) where the agreement between the two is best, we have selected the night of 29th July to 30th July for further investigation. The results are shown in Figure 6. The regression equation for this period is

$$RH = 0.9819 - 0.1153 WBD \tag{3}$$

and explains 94.5% of the data variance (adjusted R^2). The relationship is negative because a smaller dew point depression relates to more moisture.

Wet bulb depression can also be related to values of humidity numerically through the use of basic physical relationships. Dr Neville Michie provided a macro-based Excel spreadsheet which was able to calculate a variety of hydrodynamic variables (vapour pressure, saturation vapour pressure, relative humidity), given temperature, wet bulb depression, and altitude. There is a large offset between the calculated RH values and the RH values measured by the Easysense datalogger. While the Easysense values range between 48% and 70%, the RH values calculated from the wet bulb depression are all in the 70% to 80% range. This casts doubt on the precision and accuracy of the method, and calibration using an ice-point apparatus would be required to conclusively determine which measurement is at fault.

Further testing was carried out, underground, before leaving for Austria. This did not provide further calibration data, but instead served to illustrate an important equipment shortcoming: the conventional electronic relative humidity (RH) sensor employed by the Easysense datalogger package is ineffective in the high humidity environments of

24
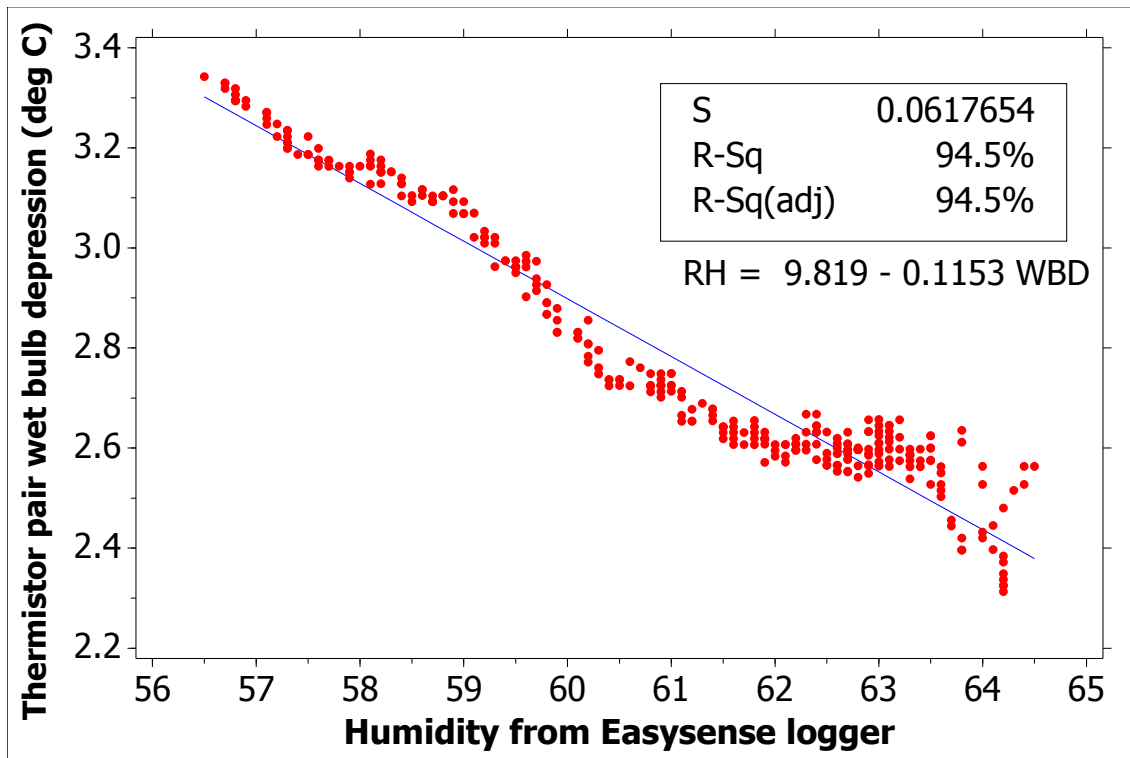
Figure 6: Linear regression of calibration data from wet / dry bulb thermistor pairs in the CUCC tackle store. The data is normally distributed (Kolmogorov-Smirnov test).

caves. On a weekend caving trip to Yorkshire, the Easysense system was deployed in the entrance of Bull Pot of the Witches, along with one HOBO datalogger and two wet / dry thermistor pairs. Figure 7 shows the response of the RH sensor. It appears to increase logarithmically to 100% (aside from an artifact at 18 minutes into the reading), and then remain at 100%. This is a commonly reported behaviour of thin-film electronic sensors, which are unreliable above 90% RH (Michie, personal communication). Failure results from condensation on the sensor surface itself. If the RH drops after a period of high RH, the sensor may take a very long time to respond, as the accumulated water must first evaporate from the sensor. Saturation behaviour was observed underground in Austria as well during a longer test, and was followed by extremely erratic behaviour (Figure 8); the readings oscillated between 0% and 100%.

The failure of the wet / dry bulb pairs to consistently match the RH sensors in the tackle store test, and the erratic behaviour of the RH sensors at high humidity necessitated a more robust, accurate humidity sensor. A "micropsychrometer" was built
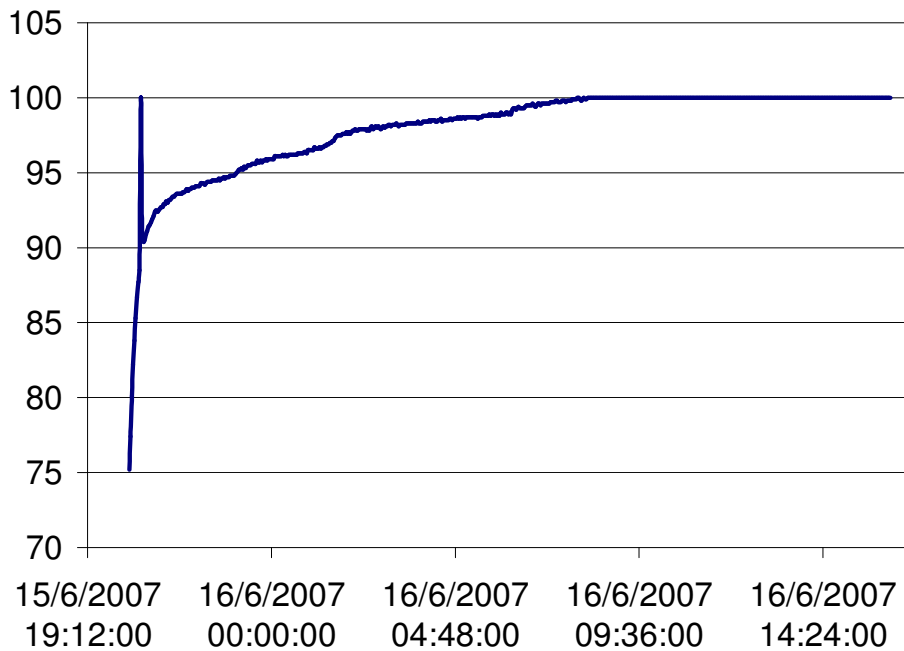
Figure 7: Unrealistic output of Easysense thin-film RH sensor in Bull Pot of the Witches, Yorkshire Dales.

to satisfy this requirement. The micropsychrometer also uses the concept of wet-bulb depression, but takes advantage of the differential heating of metals to achieve extremely precise and accurate readings. It contains three sensing elements. The first is a simple thermistor, identical to the others used in this study. The other two elements are the two ends of a thermopile. The thermopile is composed of an assembly of several fine wires known as thermocouples, created by attaching fine strands of copper wire to strands of constantin wire. A difference in temperature produces a current in the wires, which is detected by the circuitry (the Seebach effect) (Andraski & Scanlon, 2002). If one end of the thermopile (the constantin end) is kept constantly at dew point by evaporation, and the other end is kept dry (e.g., by the application of a hydrophobic substance such as WD-40) then the current between the two ends of the thermopile is related to WBD and thus humidity. Because the measurements given by the thermopile are relative rather than absolute, the thermistor is required to provide an actual temperature. A 12V DC
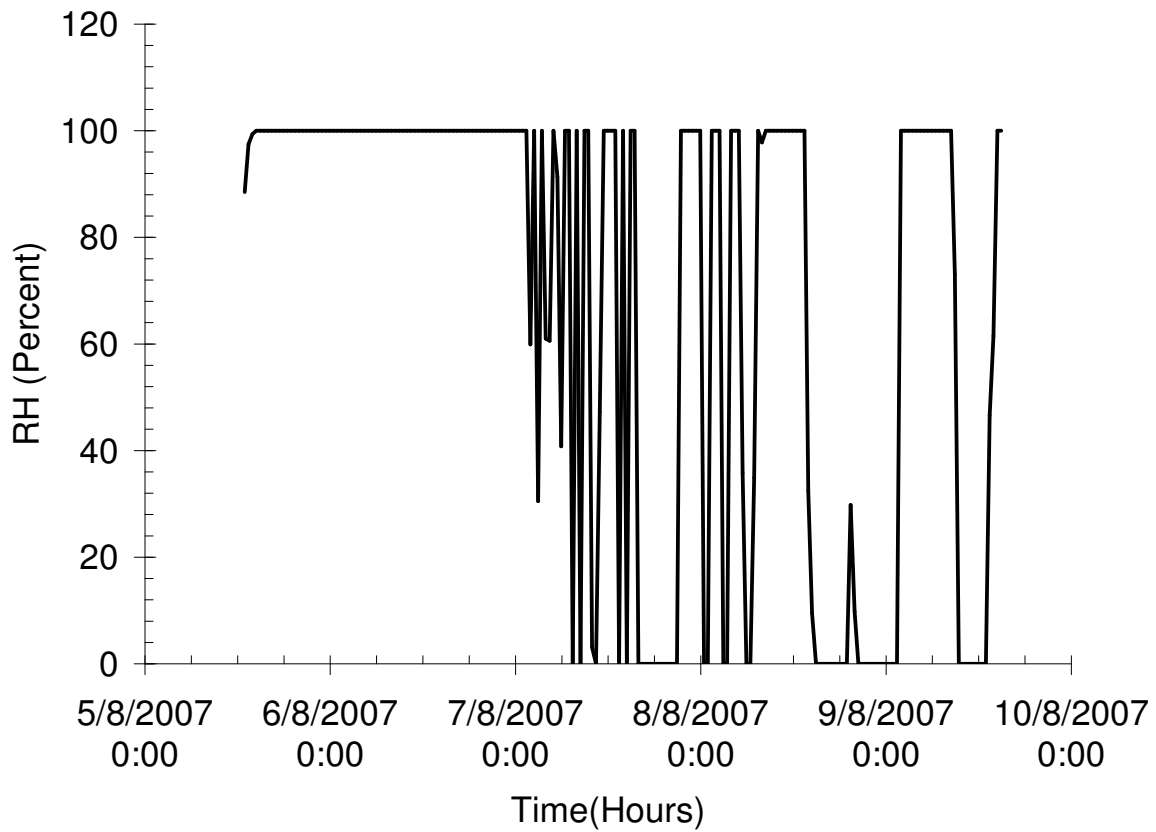
Figure 8: Unrealistic output of Easysense thin-film RH sensor in CSB passage, demonstrating the shortcomings of conventional electronic humidity sensors and the necessity for a wet / dry bulb pair solution.

fan aspirates the entire device to maintain the highest possible rates of evaporation on the wet bulb sensor and to ensure the air under investigation is from the near proximity. However, the thermocouple was broken while attaching the wet wick at the beginning of the expedition, and repair in the field proved impossible, so this is a second device which will begin producing data during the 2008 expedition.

27

4 Surface microclimate

External atmospheric characteristics are the independent variables for this study. It is important that the values used are not geographically distant, as local meteorological effects are expected to be significant. The mountainous nature of the region could cause orographic rainfall and humidity effects, valley and mountain winds, and isolation effects (Geiger, 1950) which are all intensely local in their expression. Vegetation-related surface microclimate effects are discussed in Section 5.1.1. The nearest fully-featured meteorological station with publicly available data is at Feuerkogel (47°48N 13°44E 1618m), which is around 15.6km NNW and 100m of elevation below our cave entrances (Space monitoring information support laboratory, 2008). Feuerkogel is on a slope of similar inclination and aspect, and there is one major peak between the two locations (Appendix A).
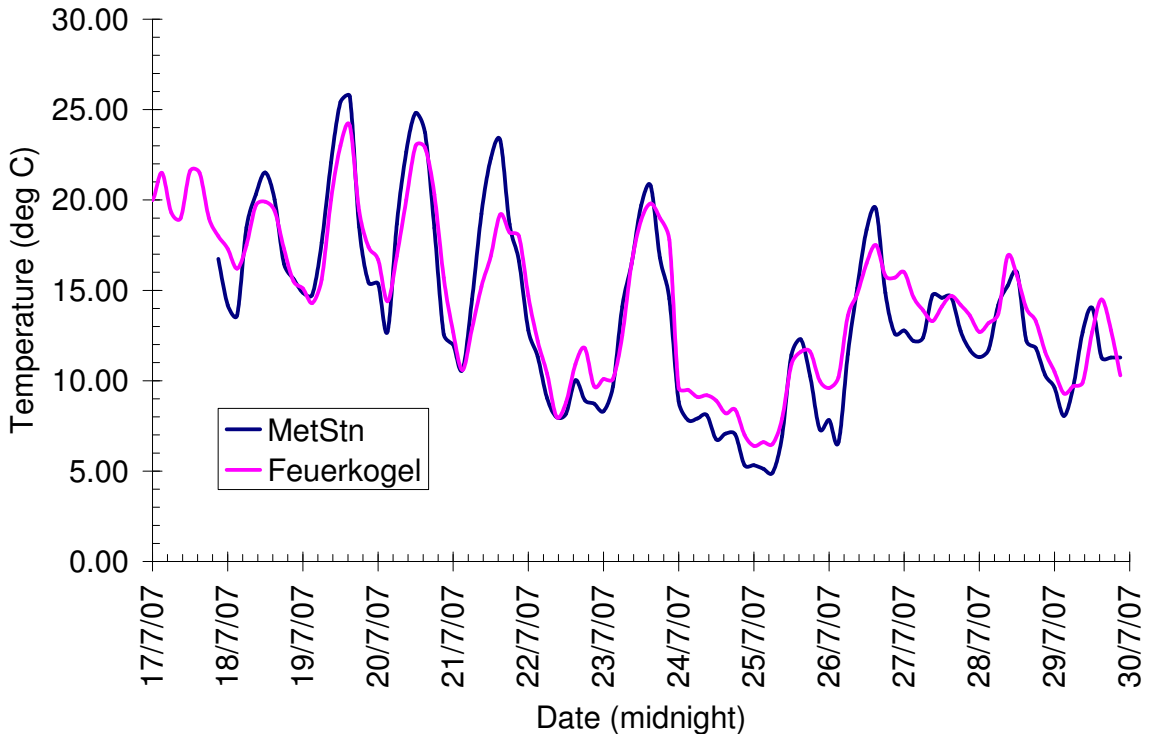
Figure 9: Comparison of surface temperatures detected by our Rundreisehöhle weather station with values from Feuerkögel.

Relating the atmospheric conditions at Feuerkogel to those recorded by our own

surface weather station informs whether Feuerkogel provides a satisfactory analogue of near-entrance surface conditions. Provided that it does, we can use Feuerkogel data to replace the data that was lost from our weather station on August 4th—16th due to a bad battery connection. Additionally, the cost and manpower required for future studies would be reduced if a weather station is not needed. Figure 9 shows the close match between our weather station's external temperature sensor and the Feuerkogel data. There does not appear to be major discrepancies between the datasets, and they have a Pearson correlation of 0.946 (P=0.00). Local effects such as those described by Schmidt (1934) appear absent.

The one noticeable difference is that the data from the study site have a greater diurnal range. Afternoon maxima are 1 to 2°C higher in six out of the nine days recorded. Although there is less discrepancy between nighttime minima, none of the Feuerkogel minima are lower than the study site, while several of the study site nights are 1 to 2°C colder. Note that our weather station data is recorded every 15 minutes, while the Feuerkogel station makes only one observation every three hours. To make the data commensurable for correlation, an Excel LOOKUP function was used to extract only the data points which correspond to times when temperature was recorded at Feuerkogel.

Instruments	From	To	Useful for study of
Rundreisehöhle			
Dry bulb thermistors (10)	15-Jul	30-Jul	Penetration length
Surface weather station	17-Jul	30-Jul	Penetration length Wind forcing
Easysense 100 datalogger (barometric pressure, temperature, RH)	15-Jul	30-Aug	N/A (data lost due to underperforming battery)
Stienbrückenhöhle: E entrance and Crowning Glory			
Wet / dry thermistor pairs (3)	04-Aug	14-Aug	Penetration length
Surface weather station			N/A (data lost due to faulty battery contact)
Observant cavers and digital cameras	6-Jul	18-Aug	Condensation droplets
Stienbrückenhöhle: CSB area			
Wet / dry thermistor pairs (4)	04-Aug	14-Aug	Humidity / Condensation
Observant cavers and digital cameras	6-Jul	18-Aug	Condensation droplets

Table 2: An overview of the data collection scheme. Does not include the micropsychrometer or sonic anemometer, which both failed to produce useful data during the study period due to malfunction and breakage.

5 Underground observations and data interpretation

5.1 Cyclical variations and penetration lengths (Q_C)

Polling of sensors in this study is on the frequency scale of minutes, and the phenomena most readily investigated are diurnal-scale processes. Is it possible to translate data on this short a scale into anything useful for decadal-scale or palaeoclimatic analysis? To answer this question, one must consider cyclical variations and penetration lengths.

There are many possible forms of external temperature and humidity variations which follow sinusoidal curves. At the human time-scale, we have diurnal and seasonal variations. Cycles of sunspots have also been identified as a cyclical component of global temperatures, and this has been correlated to cave temperatures (Stoeva & Stoev, 2005).

A Fourier transform carried out on atmospheric temperature, then, reveals a broad spectrum, with peaks in the cycle per day, year, decade, and 100,000 year ranges.

Caves can be seen to act as a frequency filter. However, the entire cave cannot be interpreted as one component for this purpose. Further into a cave entrance, there is a weaker signal from surface temperature variations and relatively slow cycles are preferentially exhibited in the cave atmosphere. To use the analogy of a low-pass capacitive filter circuit, increasing the distance into the cave is equivalent to increasing the capacitance of the capacitor in the circuit. Mathematically, this can be expressed using the concept of a penetration length x_{cycl}, defined as

$$x_{\text{cycl}} = \sqrt{\frac{a}{\pi}\tau} \qquad (4)$$

where a is thermal diffusivity $(m^2 s^{-1})$ of the cave air or limestone, and τ is the period of the forcing cycle (Badino, 2004).

Taking only cave walls into account, we can use values obtained through laboratory analysis, around $1.0\mathrm{x}10^{-6}\mathrm{m}^2\mathrm{s}^-1$. This gives the logarithmic relationship shown in Figure 10. The annual cycle (8760 hours) should disappear only 3.4m into the cave, and glacial-cycle scale influences should be extend 339m into the cave. Taking into account impurities such as water in the limestone, thermal diffusivity can be a factor of 10 higher, implying that the annual cycle would extend a more reasonable 10m into the cave.

Measurements of air temperature at distances from cave entrances have found values of penetration depth much higher than those predicted by these values of limestone thermal diffusivity. For example, Forbes (1998) detected diurnal variation in both temperature and humidity 75m into a cave. The present study found diurnal temperature variations 15 m into the cave. These cannot be accounted for by the thermal diffusivities of any of the components of the cave system. Therefore, other processes must be having a significant effect.

5.1.1 Penetration length results in Rundreisehöhle

To detect and quantify periodic trends, the timeseries data for each thermistor probe was subjected to a Fourier-transform based spectral analysis using the XLStat statistics
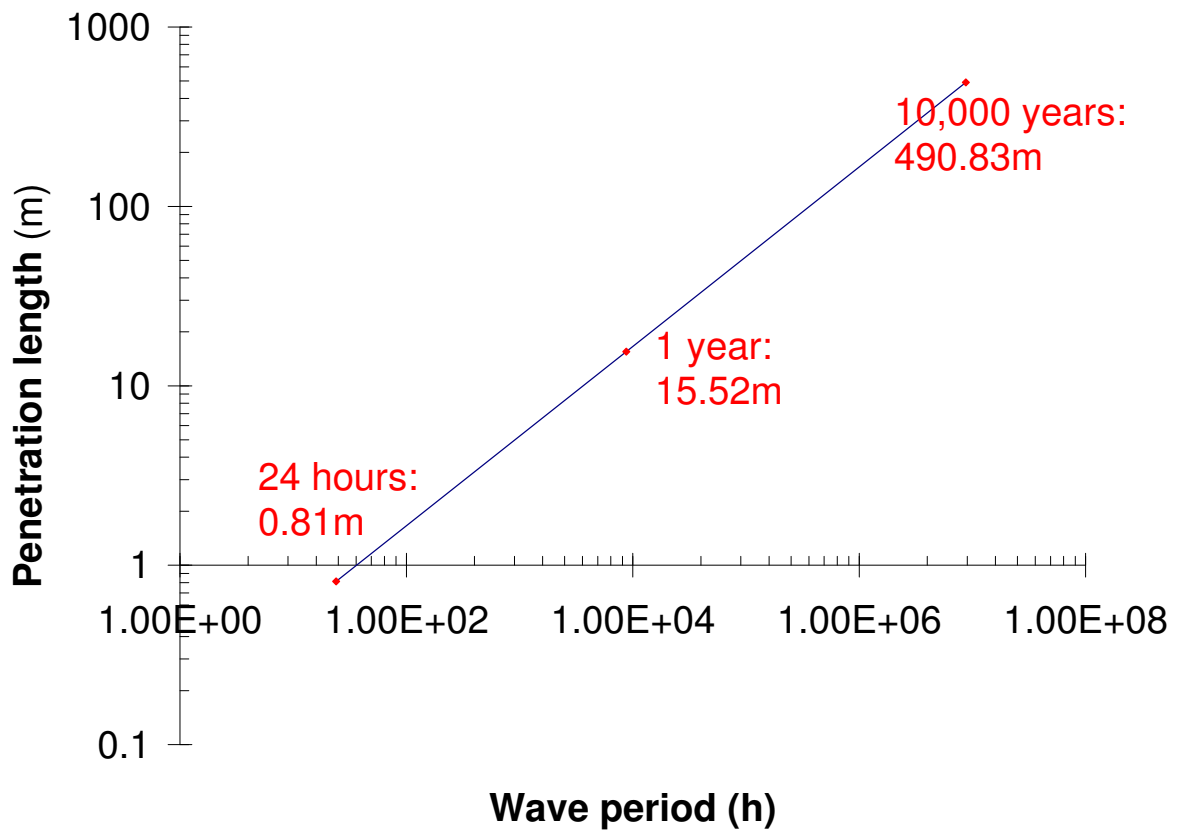
Figure 10: Penetration legnth of temperature cycles into limestone according to equation (4), taking into account only Q_C.

package for Excel, along with the contemporaneous external temperature timeseries from the weather station which was at the surface. The results suggest that at least in the case of short, well ventilated chimney caves such as Rundreisehöhle, penetration lengths far exceeded those predicted by the formula of Badino (2004).

The signals are shown in the time domain in Figure 11 . A visual appraisal of the plot suggests that there are regular, but very noisy peaks, on the diurnal scale. However, there is a clear anomaly from the beginning of the 22nd July until the beginning of the 23rd July. This anomaly was not restricted to the cave data. The weather station data suggests that a daytime storm greatly reduced the temperature peak for that day; periods of 100% humidity during that day suggest rainfall and high winds were recorded. In light of this storm action, which greatly dampened the diurnal effect for which we are testing it was decided to remove these 24 hours from the spectral analysis. Fortunately, they were at the end of the recording period, so they can be removed without risk of

interrupting the periodicity through splicing effects.
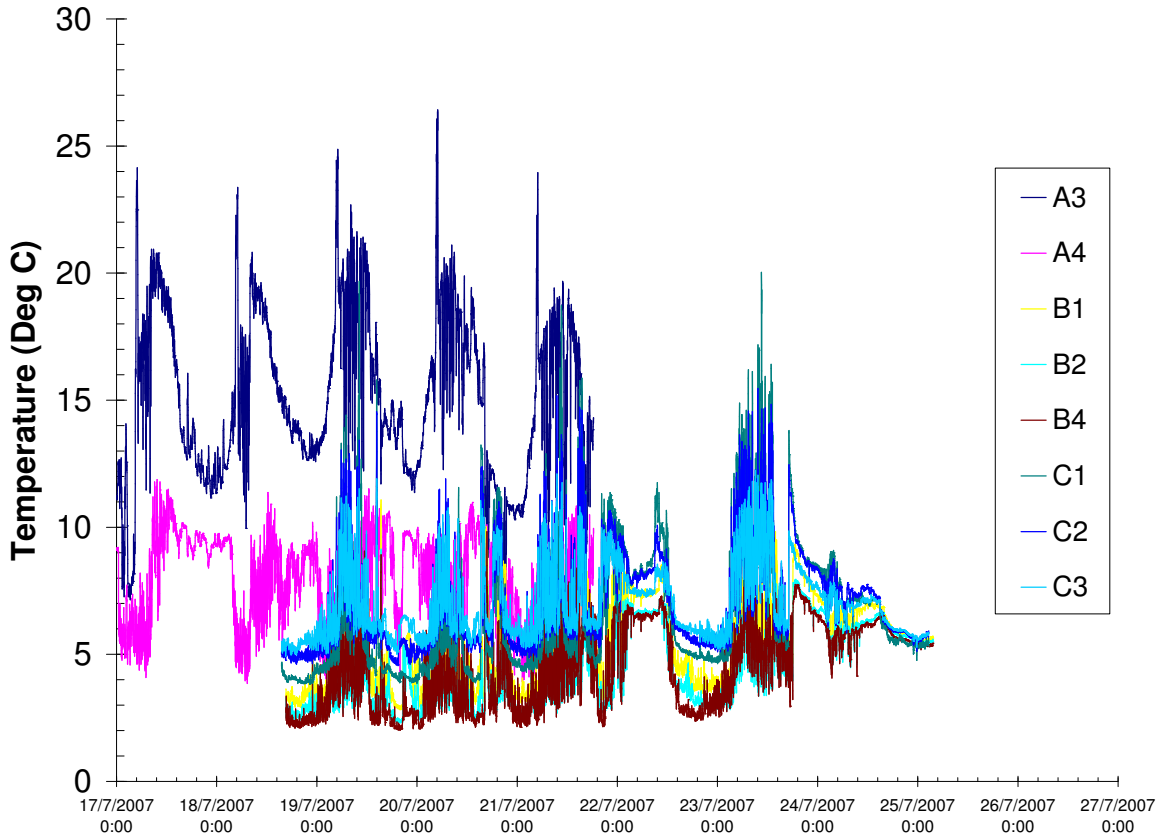
Figure 11: Temperature in Rundreisehöhle from eight thermistors. See Figure 12 for spectral analysis.

The controlling temperature oscillation, measured at the weather station (Figure 9), when converted into the frequency domain, shows a clear peak at the value 95.00 (Figure 12. Each unit, here, is one measurement. The weather station recorded temperatures once every 15 minutes, so the duration represented by a periodicity of 95 is

$$(95 \text{ readings} \cdot 15\text{min reading}^{-1})/60\text{min h}^{-1} = 23.75\text{h} \qquad (5)$$

, a value convincingly close to one day. Visual assessment confirms a daily variation with an amplitude of around 10°C. The spectrum for the weather station external temperature also trails upwards, beyond a period of about $590 \cdot 15\text{min} = 6$ days. This is a result of an overall decrease in temperature during the sampling period, and can be disregarded. Our data is insufficient to show any periodicity of that long a scale.

Because the weather station temperature sensor, at 1.5m above the ground, would
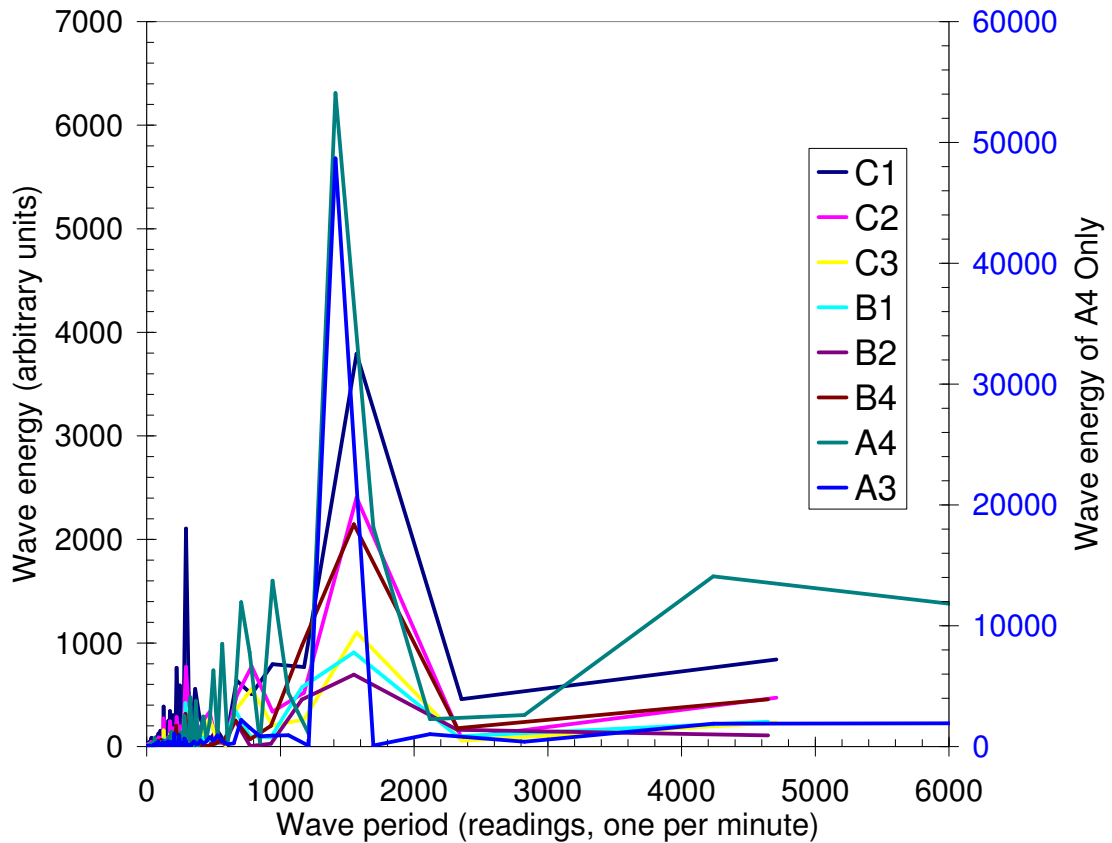
Figure 12: Fourier transform of Rundreisehöhle temperature timeseries. Time domain shown in Figure 11

not have accounted for possible temperature dampening effect of the dwarf pine which blankets the landscape above Rundreisehöhle (Figure 13), a thermistor designated A3 was placed beneath the dwarf pine canopy, just above the soil. Geiger (1950) contends that below any canopy, an "enclosed airspace" is formed, which should insulate the ground and dampen variation. Contrary to expectations of a stabilising boundary layer of trapped air, the sub-canopy sensor revealed a stronger cyclicity (amplitude of 48688 versus 10375). The peak frequency was 1412.5 readings, and like all of the Hobo thermistors, readings were taken once each minute, giving

$$\frac{1412.5}{60} = 23.54\text{h} \tag{6}$$

Like the weather station, the periodicity is slightly under a day, but close enough that we can assume the difference is due to noise in the system: elements of temperature variation outside of diurnal effects. The fact that the cyclicity is stronger underneath the

34

Figure 13: The weather station at Rundreisehöhle, also showing the dwarf pine canopy.

dwarf pine canopy could be related to the dampening of noise—the "enclosed airspace" may integrate the atmospheric signal.

Closer inspection of the timeseries reveals a notable temperature spike of 6℃ which occurs between 4:40am and 5:00am each morning. As the insolation angle changes, it seems possible that there may be a point at which light is able to filter directly through the branches and the thermistor is warmed by direct sunlight. A3 is the only thermistor to which this could conceivably occur; the weather station temperature sensor is mounted in a shielded housing and the other sensors are all below ground level.

A4 was stationed in midair roughly in the centre of the entrance plane ("drip line") for 253B. The entrance is in a depression of roughly 15m diameter, and 5m depth. Placement of A4 was achieved by hanging the cable from a convenient overhanging dwarf pine. Diurnal variation here, as might be expected, was of smaller amplitude than the weather station or the A3 (6311.15).

If the Badino (2004) conductive model of penetration length holds true for Rundreisehöhle, then we would expect diurnal variation to have a path length of 0.08m, using the standard thermal diffusivity for limestone of $1.0 \times 10^{-6} \mathrm{m}^2 \mathrm{s}^{-1}$. Our HOBO thermistors were placed three metres apart on average throughout the 25m cave (Figure 12). All six of the cave thermistors demonstrated convincingly diurnal peaks in their spectral analyses. Referring to Figure 12, we see that the peaks occur at slightly longer periods of 1549 and 1570 minutes, giving 25.8 and 26.1 hours. Again, this is probably simply due to noise in the system. It is probable that a longer sampling time would result in peaks closer to 24 hours.

The peaks do attenuate towards the centre of the cave, as shown in Figure 14, effectively an east-west transect of Rundreisehöhle where the energy of the diurnal peaks from the spectral analyses has been plotted against distance along the cave. We can investigate the nature of the relationship between diurnal amplitude and distance into the cave by fitting regressions to our data. A parabolic regression fits best, and explains 98.4% of the data (adjusted R^2), well within the 95% confidence intervals displayed on the graph.

Have we invalidated Badino's concept of penetration length? Badino himself stated that values of thermal diffusivity could be up to a factor of 10 higher for wet limestone. Although humidity data was not obtained for Rundreisehöhle, the cave subjectively felt quite wet—there was abundant damp mud and some visible condensation. The rock was fissured and fragmented, implying the presence of large, permeable pore spaces. Porewater in limestone can increase the thermal conductivity by a factor of 10. Following this, if we were to use a value of $1.0 \times 10^{-5} \mathrm{m}^2 \mathrm{s}^{-1}$ in place of $1.0 \times 10^{-6} \mathrm{m}^2 \mathrm{s}^{-1}$, the predicted penetration length increases from 0.08m to 0.8m, still far short of the diurnal variation observed 12 m into the cave.
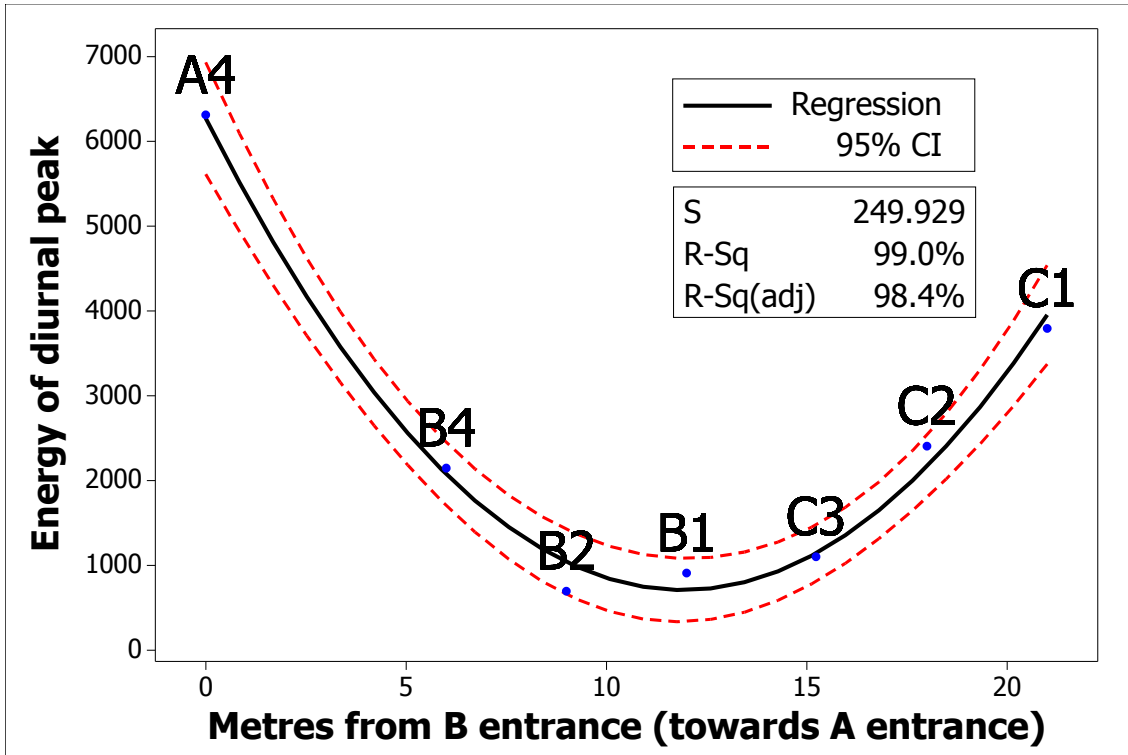
Figure 14: Amplitude of energy peak for diurnal wavelength from Fourier transform (Figure 12) for each sensor, with distance into the cave. A parabolic regression, with the equation amplitude $= 6273 - 934.8$m into cave $+ 39.26$m into cave^2 fits well. Entrances are at 0 and 25m.

The real answer to this question is that we have merely shown that Badino's formula applies to the rock, but the airspace of this cave is not forced primarily by the rock temperature. Instead, adhering to the opinions of Stoeva and Stoev (2005), the convective movement of air is probably the strongest control on our observations, rather than conduction through air or rock. Rundreisehöhle is a 30m long cave, with several metres of altitude difference between the entrances. The chimney effect (Section 5.2) likely moves a significant amount of air, carrying the external diurnal signal. Another important consideration in this situation might be the wind tunnel effect driven by external, cave-parallel wind. However, Section 5.2.1 shows that this effect is small if present at all.

5.1.2 Penetration results in Steinbrückenhöhle

Does the E entrance of Steinbrückenhöhle transmit diurnal fluctuations in the same manner observed in Rundreisehöhle? Because the Steinbrückenhöhle thermistors were polled every two minutes, we are looking for a periodicity of around

$$60\text{min} \cdot 24\text{h} \cdot 2\text{min}^{-1} \text{ reading}^{-1} = 720 \text{readings} \tag{7}$$

The dry thermistor closest to the entrance, A3, has a spectral peak which confirms this expectation, at 716.37. At roughly two metres into the cave, it does demonstrate that thermal variations are transmitted further than accounted for by Badino's "penetration length." However, it is difficult to observe a signal in the spectral analysis of next dry thermistor, a further five metres into the entrance. Visually comparing the two timeseries (Figure 15), it is difficult to deny the existence of temperature rises in the A1 data, corresponding to the marked daily peaks in A3. Restricting our Fourier analysis to the period in which these are clearest, 6th August through 9th August, gives a spectrum which shows an exceptionally strong peak, at 720.00 exactly (Table 3).

Proceeding further into the cave, we leave the entrance series and turn into Crowning Glory passage. Dynamics may be different here, as we have passed the first branching passage. However, as E entrance is still the nearest entrance by far and therefore the most likely source of diurnal variation, so the thermistors in Crowning Glory can be considered a continuation of the E entrance transect.

For the first time, the measurements appear to come from beyond the penetration length of diurnal variation. Thermistor B1 is roughly 35m from E entrance. There is in fact very little temperature variation whatsoever, and the logger has recorded a nearly constant 1.5℃. There are three notable brief spikes on the scale of 0.1 to 0.5℃. Consulting the expedition logbook, it seems probable that these spikes were caused by cavers passing the loggers on their way to other parts of Steinbrückenhöhle.

A glance at the CSB thermistor timeseries (Figure 17) is enough to show that Fourier analysis is not worthwhile. There are dips on the nights of the 10th and 11th August, and then gradual recovery until the 15th. While these dips are likely the result of outside temperature, and therefore diurnal variation might indeed be important on some days, it
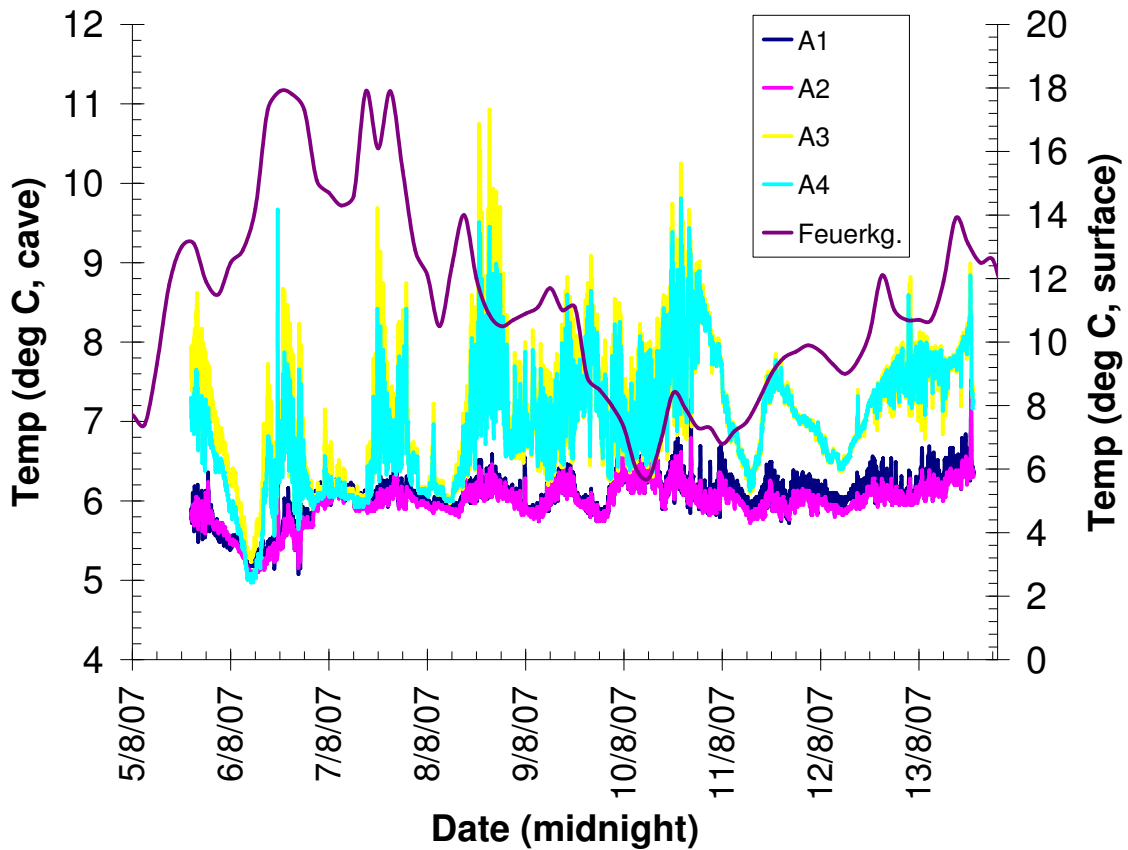
Figure 15: Temperature in E entrance area with surface temperatures from Feuerkogel.

	A3 & A4	A1 & A2	B1 & B2	B3 & B4	C1 & C2	C3 & C4
Distance from 204e entrance	4	15	35	75	150	180
Spectral analysis peak period	716.37	720	None	None	None	None
Peak amplitude	795.8	719.8	None	None	None	None

Table 3: Spectral analysis of thermistors in Steinbrückenhöhle.

is impossible to confirm the existence of a cyclicity present in only two days of a 10-day timeseries. Although we could make further visual comparisons between the surface and Steinbrückenhöhle timeseries, we risk inventing false positive linkages, as demonstrated by Wunsch (2003).

While Fourier transform spectral analysis allowed the identification of periodic fluctuations, and assessment of their relative amplitudes, we cannot convert the amplitudes to temperature. The amplitudes are incommensurable to temperature because they depend not only on the temperature range of the variation, but the degree to which that variation approaches the shape of a sine curve.
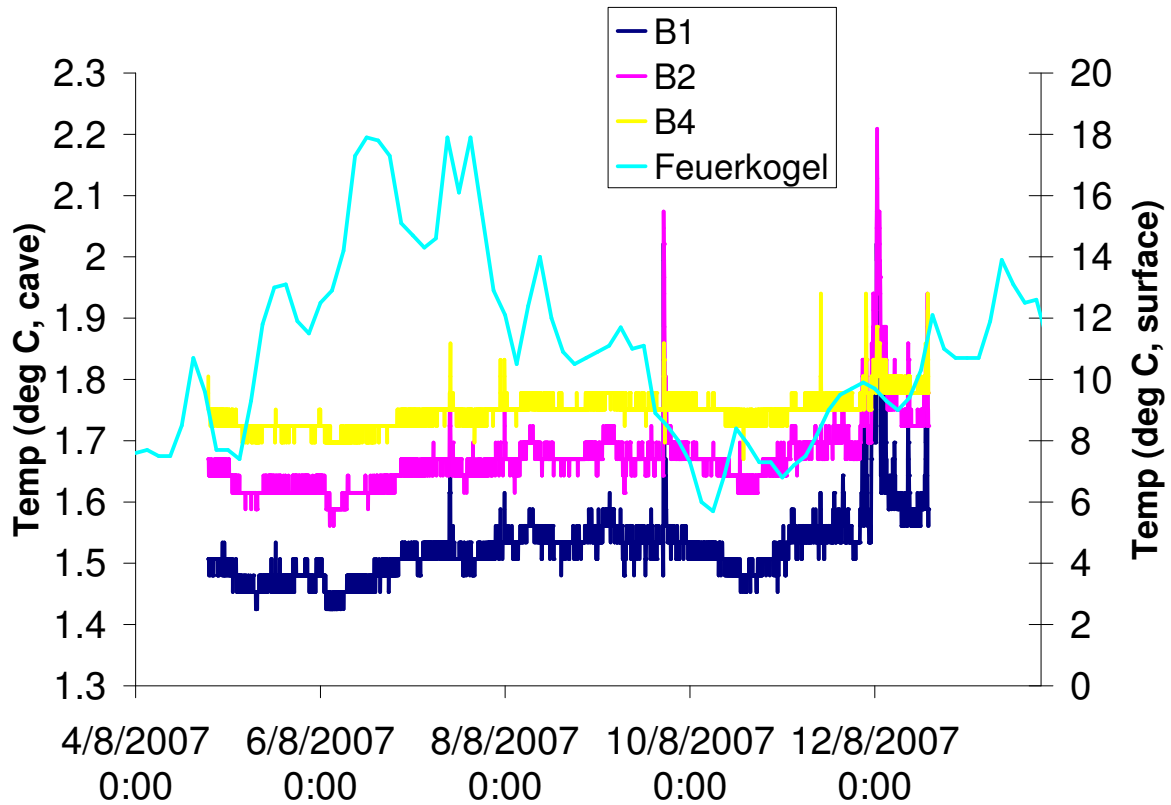
Figure 16: Temperature in Crowning Glory area with surface temperatures from Feuerkogel.

5.2 Airflow (Q_S)

Heat fluxes due to air circulation in karst massifs are frequently underestimated.

(Luetscher & Jeannin, 2004)

Airflow through caves was called the "most significant agent for transmission of external climate influence inside the caves" by Stoeva and Stoev (2005). In caves with more than one entrance, at significantly different altitudes (i.e. what Michie (1997) refers to as a Type V cave), airflow through the cave can be driven either by external wind, or a process called the chimney effect, first described by Cigna (1968). Movement of air into and out of a cave is an example of coupled heat and mass transfer, and is linked to other heat transfer processes (Figure 1). Air is also the vector for carrying water vapour (Section 5.3) and therefore enhanced airflow means not only an increased

40
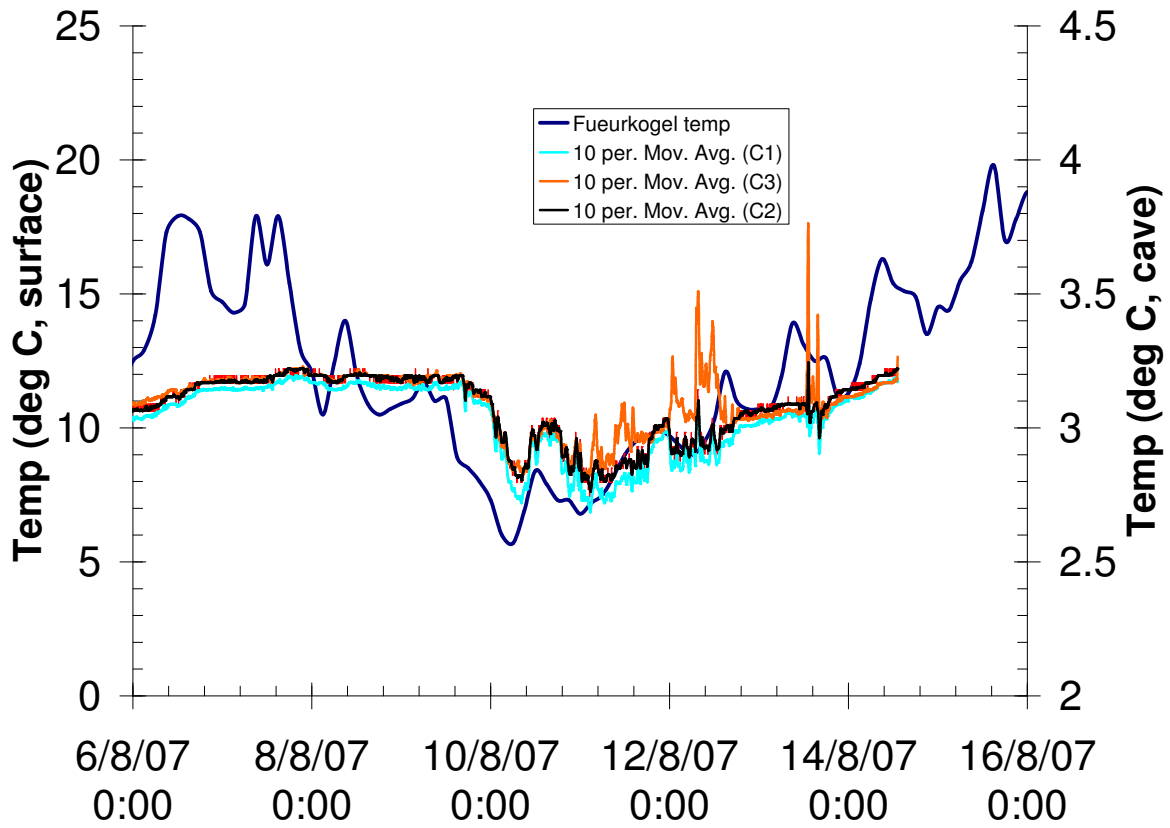
Figure 17: Temperature in CSB area with surface temperatures from Feuerkögel.

$|Q_S|$, but potentially also $|Q_L|$.

Feuerkogel 2000–08	
All year (1 March–1 March)	3.98
Summer (6 July–18 August)	11.63
Steinbrückenhöhle	
Chocolate Salty Balls	3.07
Crowning Glory Passage	1.65
Germknödel's Revenge	6.51
Rundreisehöhle	
Whole cave average	6.94

Table 4: A comparison of average temperatures (℃) for the surface and sub-surface. For practical purposes, summer is defined as the period of investigation, 6 July–18 August.

and the flow is reversed.

In the chimney effect, the difference between cave and surface temperatures drives airflow. Cave temperature is usually closer to the average annual surface temperature than the surface temperature. In the summer, as Table 4 shows, the cave is cooler than the surface, while the opposite occurs in the winter. Considering a Type V cave in the winter as a heating element with a lower and upper opening, we would expect a continuous flow of air from the lower entrance to the upper entrance. In the summer, the cave acts as a cooling element

It is worth noting that in contrast to the above comments of Luetscher and Jeannin (2004) and Stoeva and Stoev (2005), Badino (2004) states that heat fluxes associated with airflow are

small ... in comparison with the water ones

due to the much greater heat capacity of water. Indeed, most studies of caves with significant allochthonous streams indicate that the influx of water outweighs the other external influences on heat. However, the specific morphology of our caves is such that there is little water present. The caves are fossil systems resulting from the uplift of the Alps, and water does not accumulate into efficient hydrological systems until it reaches the active depth, several hundred metres below (Audra, Quinif, & Rochette, 2002). The only streamways of any significance are below -400m (Appendix B).

5.2.1 Cave-parallel wind (Rundreisehöhle)

Because Rundreisehöhle is nearly straight, we can test the influence of external, cave-parallel wind using weather station and cave thermistor data. If external wind controls air movement in the cave (rather than "chimney effect" processes outlined in 5.2), we would expect to see a temperature increase when a strong wind blows in a direction parallel to the cave, as this would increase Q_S, the advective flux of heat from the entrance of warm outside air into the cave. Rundreisehöhle runs almost exactly East-West. To extract the component of wind W_{EW} that flows either towards 90 compass degrees or 270 compass degrees, we can use the formula

$$W_{EW} = S \sin D \tag{8}$$

where S is the wind speed and D is the wind direction. For comparison,

$$W_{NS} = S \cos D \tag{9}$$

gives the N-S component of the wind.

A Pearson correlation matrix of the eight Rundreisehöhle thermistors with wind speed, N-S wind component, and E-W wind component is shown in Table 5. Overall, the indication is that cave temperatures are not controlled by surface airflow, suggesting

		A3	A4	B1	B2	B4	C1	C2	C3	Windspeed
Windspeed	Correlation	0.30	-0.10	0.09	0.12	0.22	0.11	0.18	0.14	
	P-Value	0.00	0.10	0.14	0.03	0.00	0.05	0.00	0.01	
E-W wind	Correlation	0.02	-0.16	-0.06	-0.05	-0.04	0.05	0.04	0.02	0.26
	P-Value	0.73	0.01	0.32	0.35	0.54	0.37	0.49	0.71	0
N-S wind	Correlation	-0.10	-0.29	-0.06	-0.07	-0.03	-0.04	0.01	0.00	0.39
	P-Value	0.08	0.00	0.29	0.22	0.6	0.48	0.84	0.97	0.00

Table 5: Pearson's correlation matrix of the Rundreisehöhle thermistors with windspeed, and the parallel and perpendicular components of windspeed. Autocorrelation between the three windspeed components is also shown, as are significance values.

either a lack of significant cave air movement or a dominance of the chimney effect. Correlations with p<0.05 for the wind variables occur for thermistor A4, B2, B4, C2 and C3, and A3 has one at p=0.08. A4 and A3 are the surface and entrance thermistors. It is interesting to note that A3, located in the sheltered entrance depression but outside the cave entrance, shows a fairly strong relationship with N-S wind but not E-W wind. A4, on the surface but below the dwarf pine canopy correlates with wind blowing in both directions; this is consistent with the "enclosed airspace" discussed in Section 5.1.1. Presumably this airspace is disturbed as new air enters the system with wind gusts. The remaining wind-correlated thermistors, B2, B4, C2, and C3, are correlated with wind but not cave-parallel wind.

External wind is almost certainly not a factor in Steinbrückenhöhle, where two transects of sensors were placed. Although this cave would certainly be classified as a Type V (multiple entrances at different levels, chimney effect likely) cave according to the scheme of Michie (1997), for our purposes we can think of the specific sections we are monitoring as simpler caves. The E entrance transect can be approximated as a type III cave (single entrance, descending passage), and the CSB area can be viewed as a type IV (single entrance, ascending passage). In this case we are merely considering the effect of entrances 204E and 204C on the nearby cave microclimate. It is safe to assume that at this small depth, factors such as geothermal heat flux (Badino, 2005) will not be a primary control. We do, however, need to consider the chimney effect.

5.3 Condensation (Q_L)

With regard to condensation, extensive measurements have been carried out in the caves of the Crimea and the Caucasus, reviewed by Dublyansky and Dublyansky (1998). In that paper, condensation was related to discharge of streams fed by karst aquifers, and several proposed formula for predicting underground condensation were put forth. Corrosion in association with condensation is an agent of speleogenesis and has been discussed by (Dreybrodt et al., 2005). Recently, new technologies for monitoring cave condensation are being explored (Freitas & Schmekal, 2006).

Here, we are particularly interested in the latent heat transfer (Q_L) associated with cave condensation. Michie (1997) stresses that condensation always results in a net transfer of heat from the cave air to the cave walls. However, because cave air is eventually replaced, the cave as a whole is a net recipient of heat from condensation.

5.3.1 Visual observations (Steinbrückenhöhle)

To observe condensation, expedition members were instructed to look for morphologies that suggest condensation corrosion (Dreybrodt et al., 2005). According to Jameson (2005), these include "drop dents," "rill trails," and "splash patches." However, despite 30 pairs of observant caver eyes inspecting the rock for these features, none were reported. This may not be surprising, in the light of the fact that Jameson's characteristic morphologies are only visible if they form on top of a coherent surface. Specifically, he refers to their formation on scallops, which are smooth and repetitive self-organising features formed by feedback with turbulent flowing water. Scallops are present in Steinbrückenhöhle, usually in regions with evidence of active vadose streamways such as Gösser Streamway, which was explored further during the period of study. However, as we have established above, condensation is expected near high level entrances in connection with the chimney effect. In fossil systems such as Steinbrückenhöhle, where base level lowering dominates, more shallow passages are older, and contain more breakdown material and autogenic sediment (Klimchouk, Ford, & Palmer, 2001). Passageways connecting to entrances in Steinbrückenhöhle, almost without exception, are filled with cobble to boulder size angular breakdown material in which condensation corrosion effects could

easily be obscured.

Direct, visual surveys of condensation itself proved more effective. Making use of the frequent trips to various parts of Steinbrückenhöhle, I asked expedition members to keep an eye out for any walls covered partially or completely in water droplets, and afterwards surveyed the cavers informally. Responses highlighted three main areas in which striking examples of the phenomenon were commonly observed. These three areas are shown in Figure 3. All three were near entrances, and conveniently, these happened to be in close proximity to our temperature transects—204e entrance, CSB passage, and Crowning Glory. One caver described the fields of droplets as "really pretty," while another remarked that droplets were "quite extensive" and occurred "generally on 'underside' surfaces." There was a general feeling that condensation on this scale is not typical of the UK caves in which expedition members did most of their caving, perhaps a confirmation of Dublyansky and Dublyansky (1998)'s prediction that this altitude and latitude provides better conditions for condensation than those of Britain.

Figure 18: CSB passage, with condensation droplets.

To an observer, the condensation droplets appear similar to the "reflective dots" described by Rowling (2001). Rowling holds that such droplets are not caused solely by thermodynamic phase change but that bacteria colonies of the genus *Actinomyce* encourage nucleation of condensation droplets and attract water using hydrophilic fibres. This is in accordance with the increasing realisation that bacteria are important agents in caves and that many geophysical processes which occur underground depend on microbiology, as evidenced in Barton (2006) and in a special speleological issue of Geomicrobiology Journal (v18, 2001). However, the condensation droplets that we observed do not show the features which Rowling considers indicative of the biological origin of these droplets (Figure 18). Rowling expects the droplets may exhibit a gold, yellow, or brown colour, which Moore and Sullivan (1997) attribute to presence of the pigment beta carotene in association with the actinomycetes. Additionally, bacterial droplets should be small: 0.1mm to 2mm. Because our droplets are clear and range from 4mm to 8mm, it is unlikely that this bacterial mode of formation is involved.

Following visual observations, two trips were conducted specifically for the purpose of photographing these condensation droplet fields. Figures 18 through 21 are a few examples. It is possible to roughly estimate volume of condensation from these photographs and cave survey data, which give us an idea of the surface area of the cave walls in the area. A survey tape reel was included for scale Figure 21. It is 54cm long in real life, and measuring its long axis in the image using the measure tool in Ulead PhotoImpact gives 468 pixels (px). As the tape measure is wedged against the wall behind it, it is roughly parallel to that face of rock. Droplet diameters on that face range from 4 to 8 pixels. This scales to a droplet diameter of between

$$\frac{540\text{mm}}{468\text{px}} = \frac{x\text{mm}}{4\text{px}}, x = 4.61\text{mm} \tag{10}$$

and

$$\frac{540\text{mm}}{468\text{px}} = \frac{x\text{mm}}{8\text{px}}, x = 7.70\text{mm} \tag{11}$$

If each droplet is modeled as a half-sphere, then the volume of water in each droplet is expressed by
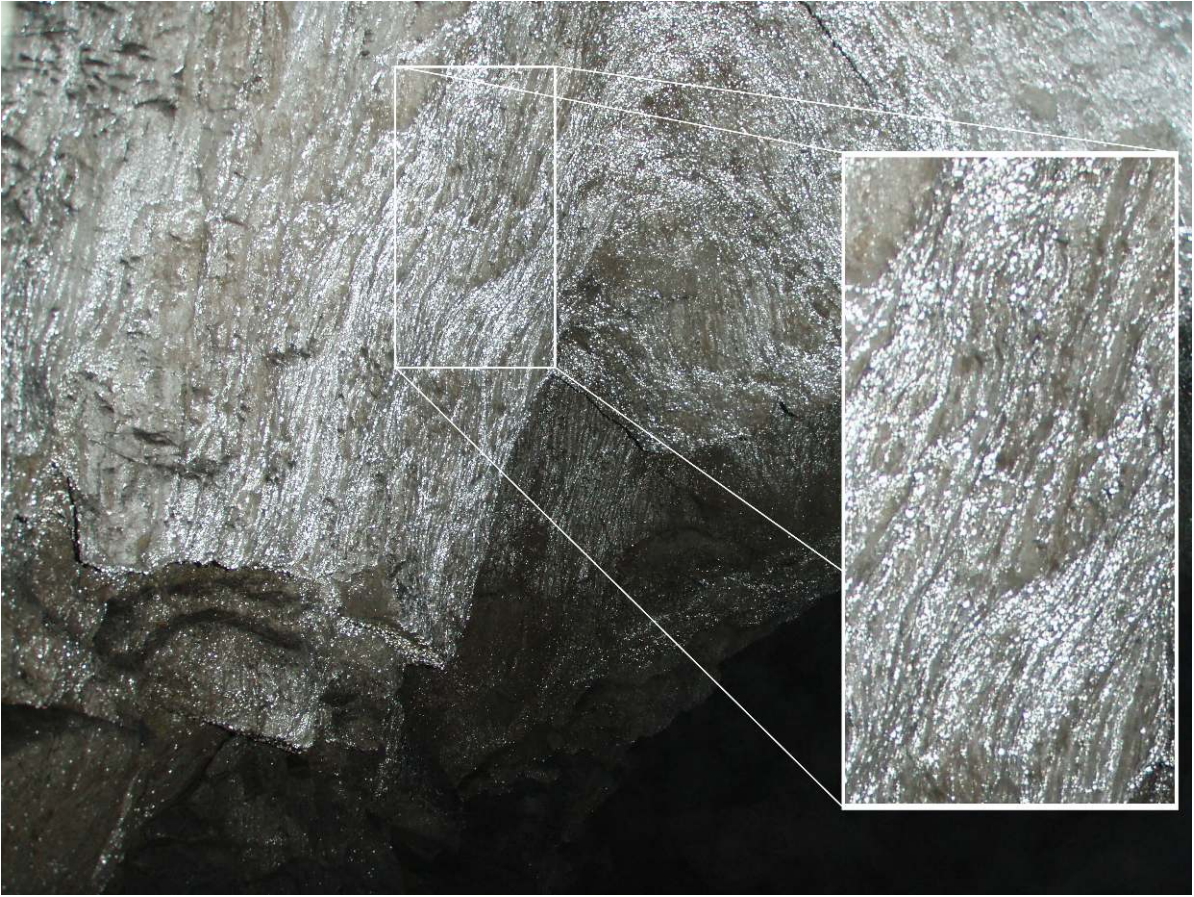
Figure 19: Condensation in Crowning Glory. Streaks detailed in inset are interpreted in the text as rivulets down which condensate slowly flows (although this is not visible on an observer's timescale.)

$$0.5 \cdot \frac{4}{3}\pi D^3 FLP \quad \begin{array}{|l|} \hline D \text{: droplet diameter} \\ \hline F \text{: droplet frequency} \\ \hline L \text{: passage length affected} \\ \hline P \text{: passage perimeter affected} \\ \hline \end{array} \tag{12}$$

$$0.5 \cdot \frac{4}{3}\pi 4.61 \text{mm} = 9.66 \text{mm}^3 = 0.00966 \text{mL} \tag{13}$$

and

$$0.5 \cdot \frac{4}{3}\pi 7.70 \text{mm} = 16.1 \text{mm}^3 = 0.0161 \text{mL} \tag{14}$$

Average droplet density is more subjective, but a reasonable estimate based on the images and firsthand observation is that there was an average of one drop every 2 to 4cm^2 . The average wall and ceiling perimeter of the affected passages based on drawn survey cross-sections is around 4m, and length of affected passages amounts to 170m (Figure 3). Therefore, we have observed roughly 188.5 L of condensate at these two

entrances.

While it is possible to make these limited guesses as to the abundance of condensed water, the actual net rate of condensation rather than the amount visible at any one time is required in order to understand the thermal effects of the condensation. The droplets in our photographs could have formed within the last hour, month, or year; we cannot distinguish between old and new droplets.

However, there are indications that the condensation process was active during our study period, and most of this condensation may have been formed each day. Closely examining Figure 20, it is clear that condensation has occurred on the Hobo datalogger in CSB passage during the period of investigation. Surveys of cavers suggest that there is a diurnal cyclicity to the formation of this condensation. The majority of reports of extensive condensation occurred in the evening; cavers noticed condensation while leaving rather than entering the cave, and one caver remarked that there was "more in the evening / afternoon." Condensation in the 204E entrance passage, Germknödel's Revenge, was observed exclusively in the evening. According to the expedition logbook, few trips were underground during the period between 2am and 10am, however, so we cannot be certain that droplets were not present then, although it seems likely due to the absence of condensation from 11am to around 2pm.

This is not entirely in accordance with the predictions put forth by (Dublyansky & Dublyansky, 1998) with the "microclimatic method" for condensation estimation. They imagine a maximum at 10am to 4pm and a minimum at 10pm to 2am, corresponding with maxima of surface temperature and humidity. However, by observing condensation droplets, we are not observing the rate of condensation, but rather the cumulative volume since the beginning of the period t. Maximum visible condensation is likely to occur at the end of the period t, which is likely to be the afternoon through early evening.

If droplets were not present in the morning, this implies that not only are condensation processes more active during the evening, but crucially that the droplets were removed from the walls by another process during the night or morning. Evaporation is one possibility. Freitas and Schmekal (2006) produced a "conceptual model" of the vapour flux between cave air and walls as a continuum, cycling sinusoidally between

Figure 20: Condensation droplets in CSB passage. Moisture on the logger (inset) demonstrates that the droplets formed during the study period.

condensation and evaporation. Besides evaporation, it is also possible that the droplets are removed by mechanical means. Gravity is the most likely culprit. The majority are attached to the underside of rock by adhesion and surface tension, and appear to be stationary, without flowing or dripping, to casual observation. However, the droplets could be moving slowly, coalescing and flowing down the side of the rock. (Dreybrodt et al., 2005) described such "flow from the rock surface down to the cave floor." Close observation of Figure 19, a photograph taken of the roof of Crowning Glory Passage, suggests this is a case. One can clearly make out vertically aligned "stripes" in the condensation pattern, presumably representing long timescale rivulets. In addition to flow down the wall through these rivulets, it has been suggested that the limestone in our area is porous enough that the droplets could flow directly into the rock and enter the pore spaces, potentially another significant pathway for mechanical removal of the condensation water (Charles Self, personal communication, 2008).

Assuming that the droplets are removed nightly by a non-evaporative process, we

Figure 21: Condensation in CSB, with tape reel for scale (54cm).

can estimate the daily latent transfer of heat to the cave walls, using water's enthalpy of condensation, which is 0.18 J g^{-1}.

$$1.885 \cdot 10^5 \text{g day}^{-1} \cdot 0.18 \text{Jg}^{-1} = 34 \text{KJday}^{-1} \qquad (15)$$

If this much condensation is occurring each day, it may be a major control on the cave wall temperature. However, this is only a first order approximation at best, and it is very likely that a significant percentage of the condensation droplets remain in the cave overnight, reducing the daily heat transfer into the cave. To determine whether the droplets are removed by flowing, dripping or by evaporation, time-lapse photography could be employed.

It is interesting that no condensation was observed on the cave floor, as one might expect the entire cross-section of the cave to behave similarly. However, as the flow modeling above (section 3.2.1) demonstrates, a cave cannot be treated as two dimensional.

The warmest air currents are most likely to contain moisture capable of condensing. These are less dense than cool, dry air, and therefore run along the top of passages. A likely explanation for the lack of condensation droplets on the floor is that the floor is in contact only with cold, dry air.

Do the observed volumes of condensation agree with either of the physical formula in Dublyansky and Dublyansky (1998) or Freitas and Schmekal (2003)? It is possible to calculate expected condensation rates using a combination of values from literature and the field data. De Frietas and Schmeckal's (2006) formula,

$$
C = (q_r - q_a)k_v
\qquad
\begin{array}{l}
C \text{ is the condensation rate in g m}^{-2}\text{ s}^{-1} \\
\hline
q_r \text{ is the specific humidity of the air in} \\
\text{g kg}^{-1}, \text{ given in equation 17.} \\
\hline
q_a \text{ is the saturation specific humidity at} \\
\text{surface temperature in g kg}^{-1}, \text{ given in} \\
\text{equation 18.} \\
\hline
k_v \text{ is an empirical transfer coefficient} \\
\text{(see text).}
\end{array}
\qquad (16)
$$

, requires little physical input due to the inclusion of k_v, the combined convective water vapour transfer coefficient. In principle, k_v is physically determined and includes a treatment of airflow rate, surface roughness and other factors. In practise, k_v appears to be empirically determined (e.g. Freitas & Schmekal, 2003). To begin with, I will test the formula with the empirically tuned value of 3.7g m^{-2} s^{-1} for k_v used in both de Freitas and Schmeckal's 2003 and 2006 studies, which they found generally applicable *"regardless of the location within the cave and ... regardless of season."* Other than k_v, the only required inputs are the specific humidity and saturation specific humidity terms q_r and q_a. Saturation specific humidity can be calculated as follows:

$q_a = 0.622\frac{e}{e_{\text{atm}}-e}$	$e_{\text{atm}} = 9.27$ hPa	Vapour pressure of external air. Calculated using daytime average temperature and RH from Rundreisehöhle weather station.
$0.622\frac{9.90}{9.27-9.90} = \mathbf{6.57}$g Kg^{-1}	$e = 9.90$ hPa	Vapour pressure of cave air. Calculated using wet / dry bulb measurements in Steinbrückenhöhle.

(17)

and

| $q_r = 0.622 \frac{e_{sr}}{e_{atm}-e_{sr}}$ | $e_{atm} = 9.27$ hPa | Vapour pressure of external air. Calculated using daytime average temperature and RH from Rundreisehöhle weather station. | (18) |
| $0.622 \frac{13.64}{9.27-9.90} = \mathbf{-1.94}$g Kg^{-1} | $e = 13.64$ hPa | Vapour pressure of cave air. Calculated using wet / dry bulb measurements in Steinbrückenhöhle. | |

Finally, we can work out that

$$C = (-1.94 - 6.57)3.7 = -31.47 \text{ g m}^{-2}\text{s}^{-1} \tag{19}$$

of condensation would occur if this formula is valid and the convective transfer coefficient used at Glowworm Caves applies. The observed Steinbrückenhöhle values of around 650g m^{-2} day^{-1} translate to 0.015g m^{-2} s^{-1}, so the estimate produced using the Frietas and Schmeckal equation is off by four orders of magnitude. Adjusting k_v to compensate would require a k_v value of 0.000008. Therefore, it seems likely that this model is not applicable to Steinbrückenöhle.

6 Conclusions and foundation for continuing research

The major conclusions reached here are:

- The difference between temperature data derived from Feuerkogel and that of our surface weather station is negligible.

- Measurements of airflow may vary up to an order of magnitude within a passage cross-section depending on the location in that cross-section.

- Neither windspeed nor the cave-parallel component of windspeed had a significant effect on temperature in Rundreisehöhle.

- Conventional RH sensors are unsuitable for cave use.

- Rundreisehöhle is entirely heterothermic, but the diurnal temperature signal attenuates towards the middle of the cave in a quadratic fashion.

- The heterothermic zone in Steinbrückenöhle extends 15 metres into E entrance. Below the entrance pitch, diurnal variations were not detectable. In CSB passage, a multi-day effect (temperature depression associated with a storm) was visible.

- Condensation in Steinbrückenöhle occurs near E entrance, in Crowning Glory passage, and at CSB. Around 200 L are visible at any one time, implying a value for Q_L of 34KJ day$^-$1. This is poorly predicted by Freitas and Schmekal (2003)'s formula.

These are the first major results from an ongoing programme of monitoring. They provide a first glimpse into the microclimatic processes coupling the surface to the subsurface which can be developed into a more comprehensive model in coming years. Strong responses to external atmospheric forcing on a diurnal timescale were seen in both Steinbrückenöhle and Rundreisehöhle. Such response is visible far enough into the cave that heat conduction through the limestone, Q_C, is relatively negligible (Section 5.1). The observations of high levels of condensation confirm Dublyansky and Dublyansky (1998)'s predictions and suggest Q_L may account for a significant warming during

the day. Measurement of airflow through the caves by the 2008 expedition using the equipment developed for this study (Section 3.2) will allow quantification of Q_S.

Now that condensation in Steinbrückenöhle's most accessible areas has been mapped, photographed, and initial estimates of condensate volume produced, the 2008 expedition can observe those areas in more detail, and expand the map to other sections of the cave, such as entrance 204A. The important question regarding the mechanism is responsible for removal of condensation droplets, and how completely they are removed on a diurnal scale, could be answered with the use of automated timelapse photography.

Confirmation that condensation occurs near entrances in accordance with the "chimney effect" (Bögli, 1980) is of interest to the exploration aims of the expedition as well as its scientific aims. Often new entrances to cave systems can be discovered from below. If condensation can be treated as a reliable indicator that an entrance is nearby, then explorers hunting for entrances (such as CUCC in Tunnockschacht, a cave of which 3km has been explored via a single entrance) can increase theias well asr chances of success by keeping an eye out for water droplets.

Because this is a multi-year project, annual cycles as well as the diurnal timescale will be observed. At the end of Summer 2007 data collection, I installed a datalogger attached to a four thermistor transect with 50m spacing between thermistors in CSB. The datalogger will record the temperature at four points, once an hour, until the memory fills up in July 2008, when it will be downloaded by CUCC expedition members. CSB did not show coherent diurnal temperature variation (Figure 17). If it does demonstrate an observable annual cycle of temperature variation, this will support the "frequency filter" theory that longer periodicities are observed further into the cave (Section 5.1), which would allow researchers to select speleothem for analysis from favourable locations. Note that this possibility applies only to investigations of allochthonous climate proxies, rather than proxies relying on surface signals such as humic / fulvic acids or $\delta_1 8O$ forced by percolation water.

Another interesting possibility is that the 12 month dataset will suggest entirely different processes are dominant in the winter. Luetscher, Lismounde, and Jeannin (in press) found that in a cave system in Switzerland, similar to Steinbrückenöhle, there is a

seasonal shift between "open" and "closed" regime with seasons. Most of the entrances to Steinbrückenhöhle are partially or entirely closed by snowfall during the winter, reducing airflow. If Q_S is a major factor, then we would expect to see a "flattened" curve and less overall subsurface-surface heat transfer.

Future studies will benefit from the equipment developed, the challenges encountered, and the methodology employed in addition to the conclusions themselves. Section 3.3 confirms beyond all reasonable doubt Michie (1997)'s contention that conventional RH sensors are useless in caves. It also suggests that non-aspirated wet / dry bulb pairs may be inadequate as they failed to match either calculated or RH values (Figure 5). Our temperature monitoring system can be highly recommended, and after repairs and improvements the micropsychrometer and ultrasonic anemometers constructed for the 2007 expedition should produce useful data in 2008.

References

Andraski, B., & Scanlon, B. (2002). Thermocouple psychrometry. *Methods of soil analysis. Part*, *4*, 609–642.

Audra, P., Quinif, Y., & Rochette, P. (2002). The genesis of the tennengebirge karst and caves (salzburg, austria). *Journal of Cave and Karst Studies*, *64*(3), 153-164.

Auler, A., & Smart, P. (2004). Rates of condensation corrosion in speleothems. *Speleogenesis and Evolution of Karst Aquifers*, *2*(2).

Badino, G. (2004). Cave temperatures and global climatic change. *Int. J. Speleol*, *33*(1/4), 103-114.

Badino, G. (2005). Underground drainage systems and geothermal flux. *Acta Carsologica*, *34*(2), 277–316.

Baker, A., Asrat, A., Fairchild, I. J., Leng, M. J., Wynn, P. M., Bryant, C., et al. (2007). Analysis of the climate signal contained within d18o and growth rate parameters in two ethiopian stalagmites. *Geochimica et Cosmochimica Acta*, *71*(12), 2975-2988.

Barton, H. A. (2006). Introduction to cave microbiology: a review for the non-specialist. *Journal of Cave and Karst Studies*, *68*(2), 43-53.

Bögli, A. (1980). *Karst Hydrology and Physical Speleology.* Springer-Verlag.

Campbell, G., & Unsworth, M. (1979). An Inexpensive Sonic Anemometer for Eddy Correlation. *Journal of Applied Meteorology*, *18*(8), 1072–1077.

Chapman, P. (1993). *Caves and Cave Life.* HarperCollins.

Cigna, A. (1968). Air circulation in caves. *Fourth international speleological congress, proceedings*, *3*, 43–49.

Dreybrodt, W., Gabrov Ek, F., & Perne, M. (2005). Condensation corrosion: a theoretical approach. *Acta Carsologica*, *34*(2), 317-348.

Dublyansky, V. N., & Dublyansky, Y. V. (1998). The problem of condensation in karst studies. *Journal of Cave and Karst Studies*, *60*(1), 3-17.

Fairchild, I. J., & McMillan, E. A. (2007). Speleothems as indicators of wet and dry periods. *International Journal of Speleology*, *36*(2), 69-79.

Fairchild, I. J., Smith, C. L., Baker, A., Fuller, L., Spötl, C., Mattey, D., et al. (2006).

Modification and preservation of environmental signals in speleothems. *Earth Science Reviews*, *75*(1-4), 105-153.

Fernández-Cortés, A., Calaforra, J., Jiménez-Espinosa, R., & Sánchez-Martos, F. (2006). Geostatistical spatiotemporal analysis of air temperature as an aid to delineating thermal stability zones in a potential show cave: Implications for environmental management. *Journal of Environmental Management*, *81*(4), 371–383.

Forbes, J. (1998). Air temperature and relative humidity study: Torgac cave, new mexico. *Journal of Cave and Karst Studies*, *60*(1), 27-32.

Freitas, C. de, & Schmekal, A. (2003). Condensation as a microclimate process: measurement, numerical simulation and prediction in the Glowworm Cave, New Zealand. *International Journal of Climatology*, *23*(5), 557-575.

Freitas, C. de, & Schmekal, A. (2006). Studies of condensation/evaporation processes in the glowworm cave, new zealand. *International Journal of Speleology*.

Geiger, R. (1950). *The Climate Near the Ground, translated by MN Stewart et al.* Harvard Univ. Press, Cambridge, Massachusetts.

Hall, K., Meiklejohn, I., & Arocena, J. (2007). The thermal responses of rock art pigments: Implications for rock art weathering in southern Africa. *Geomorphology*, *91*(1-2), 132–145.

Heaton, T. (2005). Caves, a tremendous rance of energy environments on earth. *NSS News*, *44*, 301-304.

Jameson, R. (2005). Modification of scallops by condensation corrosion in snedgar's cave, west virginia, usa. *2005 Salt Lake City Annual Meeting*.

Kennedy, J. (1998). Pre and post gate microclimate monitoring. *Bat Conservation International. March*, 216-224.

Klimchouk, A., Ford, D., & Palmer, A. (2001). *Speleogenesis: evolution of karst aquifers*. The National Speleological Society.

Lauritzen, S., & Lundberg, J. (1999). Calibration of the speleothem delta function: an absolute temperature record for the Holocene in northern Norway. *The Holocene*, *9*(6), 659.

Lomas, C., & Korman, M. (1990). Fundamentals of Hot Wire Anemometry. *The Journal*

of the Acoustical Society of America, *87*, 1379.

Luetscher, M., & Jeannin, P. Y. (2004). Temperature distribution in karst systems: the role of air and water fluxes. *Terra Nova*, *16*(6), 344-350.

Luetscher, M., Lismounde, B., & Jeannin, P. Y. (in press). Heat exchanges in the heterothermic zone of a karst system: Monlesi ice cave, swiss jura mountains. *Journal of Geophysical Research*.

Michie, N. (1997). *An Investigation of the Climate, Carbon Dioxide and Dust in Jenolan Caves, N.S.W.* PhD in Earth Sciences, Macquarie University.

Moore, G., & Sullivan, G. (1997). *Speleology: Caves and the Cave Environment.* Cave Books.

Oke, T. (1998). *Boundary Layer Climates.* Methuen.

O'Neil, J. R., Clayton, R. N., & Mayeda, T. K. (1969). Oxygen isotope fractionation in divalent metal carbonates. *The Journal of Chemical Physics*, *51*(12), 5547-5558. Available from `http://link.aip.org/link/?JCP/51/5547/1`

Rowling, J. (2001). *Cave entrances - reflective dots* [web page]. World Wide Web electronic publication. Available from `http://www.speleonics.com.au/jills/byzone/byzoneReflDots.html`

Schmidt. (1934). Observations on local climate in austrian mountains. *Quarterly Journal of the Royal Meteorological Society*, *60*, 345-352.

Space monitoring information support laboratory. (2008). *Russia's weather database server* [web page]. Available from `http://meteo.infospace.ru/`

Spötl, C., Fairchild, I. J., & Tooth, A. F. (2005). Cave air control on dripwater geochemistry, obir caves (austria): Implications for speleothem deposition in dynamically ventilated caves. *Geochimica et Cosmochimica Acta*, *69*(10), 2451-2468.

Stoeva, P., & Stoev, A. (2005). Cave air temperature response to climate and solar and geomagnetic activity. *Memorie della Societa Astronomica Italiana*, *76*, 1042.

The present author. (2007). Science and surveying: Totes gebirge, austria 2007. *Speleology: The Bulletin of British Caving*, *11*, 6-10.

Verheyden, S. (2005). Trace elements in speleothems: a short review of the state of the art. *Speleogenesis and Evolution of Karst Aquifers*, *3*(1).

Wunsch, C. (2003). Greenland—Antarctic phase relations and millennial time-scale climate fluctuations in the Greenland ice-cores. *Quaternary Science Reviews*, *22*(15-17), 1631–1646.

A   Relative location of Feuerkogel

B   Study area maps

C   Anemometer construction